UNIVERSITY OF COPENHAGEN
FACULTY OF SCIENCE

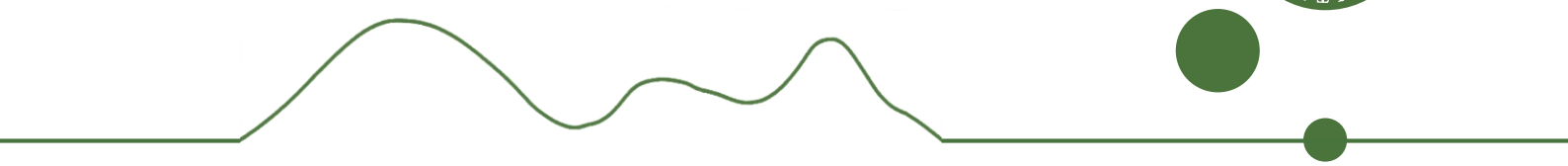

Master's thesis

The Effect of Anesthetics on Phase Transitions in Biological Membranes

Tea Mužić

Supervisor:
Thomas Heimburg

Niels Bohr Institute
Faculty of Science
University of Copenhagen

Submitted: May 31st, 2016

Acknowledgments

First of all, I would like to thank my supervisor, Thomas Heimburg for the trust he put in me by giving me the opportunity to work on this exciting project. I thank him for mentoring and shaping me both as a scientist and as a person, and giving me opportunities to develop even outside the scope of the thesis, from teaching experience, collaboration with Herlev Hospital, to recognizing my work as worth of publication.

I would like to thank Membrane Biophysics group members:

Foremost, Fatma, for introducing me to the lab and being a partner in crime for the first set of experiments.

A huge thank you to Henrike, Karis and Tian for whole-heartedly sharing their time and knowledge, guiding me and advising me through challenges and, finally, making sure that we go for lunch on time.

And of course, rest of the group, Sidsel, Rima, Vardan, Nobutake, Alfredo and Viktor. Thank you for being a source of interesting questions, discussions, as well as many answers.

I thank First year project students Estrid, Asla, Isabella and Cecilie for perseverance and diligence in producing the lipid set of experiments.

Thank you to K building staff and students for great atmosphere, fun lunch times and hang outs on and off the campus, which made long hours at the office feel like home.

Special thanks go to my friend Dafne who let me exploit her degree in English and love for reading by making her go through manuscripts of this thesis. Thank you for your time and support.

Lastly, I would like to thank my family for unconditional love and support. Thank you for believing in me and letting me explore life to the fullest.

Abstract

Our coherent interaction with our surroundings can be attributed to our nervous system. Immense research focused on the nature of signal propagation in the system, over the course of history, has yielded several models. The work presented here has been done in the context of the Soliton model which ascribes the nature of the signal propagation to solitons, i.e. electro-mechanical waves.

The intention of this thesis was to investigate, for the first time, the influence of anesthetics on the complex phase transitions in biomembranes. A big part of this thesis was dedicated to the development and the optimization of methods for sample preparation. Differential scanning calorimetry experiments were done on sheep and pig spinal cord samples in presence of anesthetics. The obtained results show that anesthetics change the membrane properties by shifting the gel - fluid phase transition of the lipids.

The 30 ECTS thesis is submitted to fulfill the requirements for M.Sc. in Physics at the Niels Bohr Institute, Faculty of Science, University of Copenhagen, Denmark. The experimental work was conducted at the Niels Bohr Institute, University of Copenhagen.

Table of contents

1 Introduction

1.1 The cell

A cell is the smallest structural, functional, and biological unit of all known living organisms. It is often called the "building block of life". Their dimensions span from 1 to 20 µm. Each cell is surrounded by a membrane also known as plasma membrane. Organelles within the cell are individually enveloped by 5 to 8nm thick membranes. [1] Membranes act not only as the physical boundary of a cell but also as a functional barrier that prevents ions and nutrients form diffusing and, at the same time, allows intake if the same are needed.

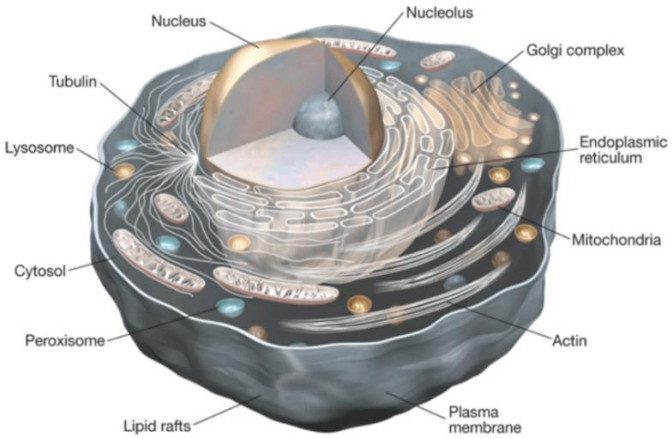

Figure 1: Illustration of the outer membrane and inner organelles of a mammalian cell. [32]

Cells's most important building blocks are nucleic acids, proteins, ribosomes and lipids. Nucleic acids, namely, ribonucleic acids (RNA) and deoxyribonucleic acids (DNA) are carriers of information. Proteins on the other hand, like enzymes, transport proteins and receptors, are carriers of function in the cell. Ribosomes are key elements in protein synthesis and finally lipids are a fatty components that due to their natural tendency form membranes. [1]

1.2 Biological membranes

The cell membrane is primarily composed of a lipid bilayer with proteins of various functions embedded within the membrane (Figure 2). The mass ratio between lipids

and proteins is typically 1 with variations between different membranes from 0.25 up to 4 [2]. Myelin, the fatty white substance that surrounds the axon of some nerve cells, for example, is characterized by a high proportion of lipid (70 to 85%) and, consequently, a low proportion of protein (15 to 30%) [3]. With proteins being attached to the bilayer in different configuraion, the in-plane membrane is mainly occupied by lipids [4].

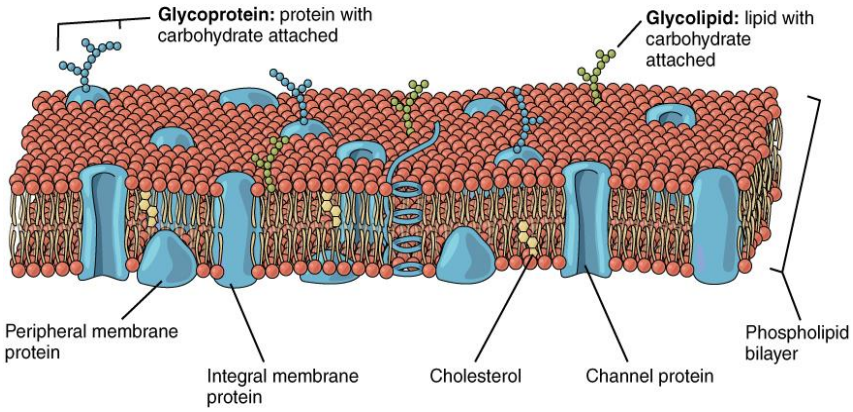

Figure 2: Illustration of the cell membrane [33]

In biological membranes a variety of lipids could be found. They are classified as sterols, sphingolipids and phospholipids. Phospholipids are most abundant species of lipids in plasma membranes. Phosphate-containing head group and two hydrocarbon chains are linked by a glycerol backbone. Their head is polar and tail apolar, making those parts hydrophilic and hydrophobic, respectively. Due to their amphiphilic characteristic, in contact with water lipids tend to form structures like bilayers, exposing the head groups to the water and shielding the hydrocarbon chains.

Lipids differ in net charge, size, polarity and degree of saturation. Their structure varies across the different cell types and is influenced by the physiological conditions at which cell has grown. [1]

1.3 Membrane phases and transition

Lipid bilayers can be found in a number of different phases. Phases are classified by the lateral ordering of the head groups and ordering of the lipid chains. Presented below are three phases in order of their thermal presence, from lower to higher temperatures:

THE SOLID - ORDERED (GEL) PHASE is a phase with highest packing density. Entropy is low with head groups being arranged in a solid triangular lattice and chains being in fully stretched.

THE RIPPLE PHASE is a state of membrane between two transitions where membrane surface displays periodical "ripples" of ordered phase within disordered lipids. If secondary biomolecules are present, this phase is not observed. This indicates that this phase rarely occurs in biological membranes. [5]

THE LIQUID - DISORDERED (FLUID) PHASE exhibits loss in lattice structure and chain order. The enthalpy is higher compared to a gel phase. Lipids randomly move within 2-dimensional lattice. In this state the area of the lipid membrane is 24% larger while the thickness is 16% smaller than in the gel phase.[6]

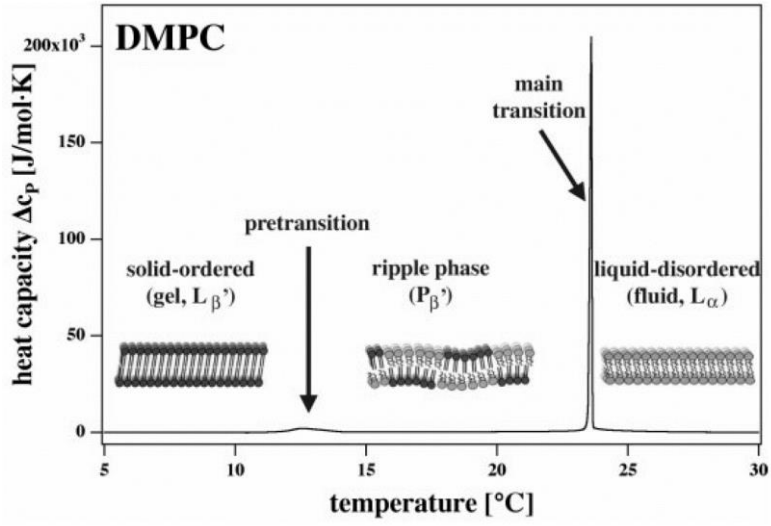

Figure 3: Melting profile of dimyristoyl phosphatidylcholine DMPC. Three distinct regions, separated by transitions peaks, are accompanied with illustrations of corresponding lipid phases. [1]

Figure 3 displays a heat capacity profile of synthetic lipid membrane DMPC. There are two phase transitions, pre- and main-transition.

In heat capacity profiles of biological membranes, the main lipid transition is the one of biological relevance. It is found in proximity to the physiological temperature of the organism. Since the position of the transition depends on different thermodynamical parameters, this potentially gives the system a mean to respond the environmental changes and regulate behavior of the membrane.

2 Nerve Pulse Propagation

Our coherent interaction with our surroundings can be attributed to our nervous system, which receives signals from the brain in the matter of milliseconds. Throughout history, immense research has been focused at understanding the nervous system. The comprehension of the nature of the propagation of the signal in its building block, the nerve, would not only enable us to understand the phenomenon, but also become one step closer to understanding how brain functions as a whole.

Two different approaches have been used to model nerve pulse propagation. Hodgkin and Huxley model, the first of the two, is the textbook electrical model for the propagation of nerve signal formulated by Alan L. Hodgkin and Andrew F. Huxley in 1952 [7]. The second model, proposed by Thomas R. Heimburg and Andrew D. Jackson in 2005 [8], ascribes the nature of the signal propagation to solitons, electromechanical waves.

2.1 The Hodgkin-Huxley Model

Although known and measured before, the action potential - the electric nerve signal, was described for the first time by Hodgkin and Huxley. They ascribed it to ions passing through the membrane via protein ion channels.

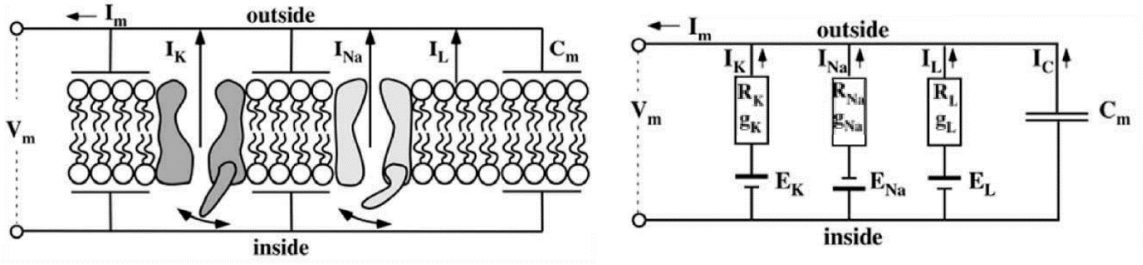

Figure 4: Schematic representation of a membrane (left) and equivalent electric circuit (right). Subscripts K, Na and L stand for potassium, sodium and leak respectively. [1]

As seen in Figure 4, proteins play the role of ion channels (selective for potassium K^+ and sodium Na^+) and contribute to the circuit as resistors. Their conductance is voltage and time dependent. The lipid membrane, because of its hydrophobic interior, is modeled as an insulator with fixed membrane capacitance. The total current I_m through the membrane is thus a sum of ionic currents through proteins and capacitive currents due to the lipid bilayer:

$$I_m = g_K\ V_m, t \quad V_m - E_K\ + g_{Na}\ V_m, t \quad V_m - E_{Na}\ + C_m \frac{dV_m}{dt} \qquad (1)$$

Here, $g_{K,Na}$ are the conductances of the potassium and sodium channels, V_m is the transmembrane voltage, $E_K \approx -70\ mV$ and $E_{Na} \approx +30\ mV$ are resting potentials, and C_m is the membrane capacitance. The resting potential value for each ion species is the voltage at which no net flow of the ion occurs. It depends on the difference in ion concentration on the two sides of the membrane.

Although widely accepted, this model has some shortcomings. The dependence of conductance on voltage and time in Hodgkin and Huxley model is fitted to match the experiments. Moreover, the model also fails to explain some of its thermodynamical consequences. If the system acts as an electric circuit, heat should be released upon ions flow through the channels (resistors). It has been shown that this is not the case. Heat is fully reabsorbed indicating that the system undergoes a reversible adiabatic process. [9] Furthermore, the model assumes constant capacitance since thickness and composition of the excitable membrane were unknown at the time. [7] However, today it is known that the capacitance can be influenced by structural changes of membranes. [10] The melting transition of a biological membrane, which is just a couple of degrees lower than the physiological temperatures, could be one of the sources of those changes. [8] Additionally, voltage could be one of the variables affecting the temperature at which biological membranes melt.

2.2 The Soliton model

In the need of including thermodynamical variables in the modeling of the action potential that are lacking in the pure electrical representation, the Soliton model was proposed by Heimburg and Jackson in 2005. Describing nerve signals as solitons, self-reinforcing solitary electro-mechanical waves, would explain the origin of some of the experimentally observed phenomena, like the adiabatic nature of nerve pulses, the electrical and mechanical nature of nerve signals and the effect of anesthetics.

The requirement for soliton existence is nonlinear and dispersive (frequency dependent) medium. In biological membranes both requirements are fulfilled. [8]

If we approximate a nerve to a one-dimensional cylindrical membrane, sound propagation is governed by equation:

$$\frac{\partial^2}{\partial t^2}\Delta\rho^A = \frac{\partial}{\partial x}\left(c^2\frac{\partial}{\partial x}\Delta\rho^A\right) \tag{2}$$

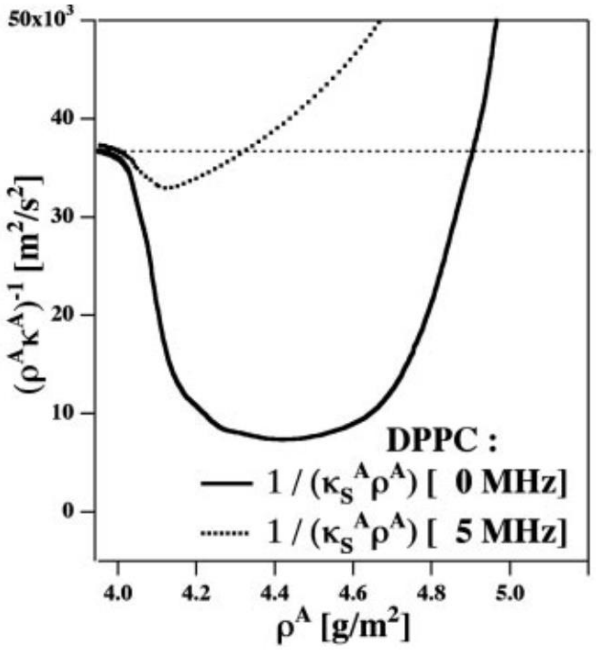

Figure 5: Experimental measurement of the speed of sound as a function of membrane area density for large unilamellar vesicles of DPPC. [8]

Here, c is the speed of sound and $\Delta\rho^A = \rho^A\ x,t\ - \rho_0^A$ is lateral density of the membrane. Figure 5 demonstrates that both requirements for soliton existence are fulfilled. The speed, close to the melting transition, is a nonlinear function of density and function of frequency.

Nonlinearity of the speed of sound could be captured by $c^2\ \Delta\rho^A = c_0^2 + p\ \Delta\rho^A + q\ \ \Delta\rho^{A\ 2} + \cdots$ and dispersion term approximated by $-h\frac{\partial^4}{\partial x^4}\Delta\rho^A$. Where c_0 is sound velocity in the fluid state, p and q are Taylor expansion coefficients and h is a dispersion constant. One arrives at:

$$\frac{\partial^2}{\partial t^2}\Delta\rho^A = \frac{\partial}{\partial x}\left(c_0^2 + p\ \Delta\rho^A + q\ \ \Delta\rho^{A\ 2}\ \frac{\partial}{\partial x}\Delta\rho^A \right) - h\frac{\partial^4}{\partial x^4}\Delta\rho^A \qquad (3)$$

For $\Delta\rho^A\ x,t\ = \Delta\rho_0^A\ e^{i\omega\ t - x/c_0}$ dispersion term in (3) takes the form $c^2\ \omega\ = c_0^2 + hk^2 \approx c_0^2 + h\frac{\omega^2}{c_0^2}$ which is the lowest order, non-trivial, expansion of the speed of sound frequency dependence.

The analytical solution [11] of (3) is:

$$\Delta p^A\ z\ = \frac{p}{q}\frac{1 - \left(\frac{v^2 - v_{min}^2}{c_0^2 - v_{min}^2}\right)}{1 + \left(1 + 2\sqrt{\frac{v^2 - v_{min}^2}{c_0^2 - v_{min}^2}}\ \cosh\left(\frac{c_0}{h}z\sqrt{1 - \frac{v^2}{c_0^2}}\right)\right)} \qquad (4)$$

with $v_{min} = \sqrt{c_0^2 - \frac{p^2}{6\ q}}$ being the minimum group velocity.

The model predicts a minimum velocity of solitons in membranes that, for DPPC lipid membranes, yields a number which is very close to the velocity measured in myelinated nerves. Furthermore, it has also been shown that the Soliton model is

not affected by noise and heterogeneities of the membrane. The signal can be triggered by non-solitonic excitation of a sufficient amplitude. This is essential to describe the conditions in biomembranes. [11]

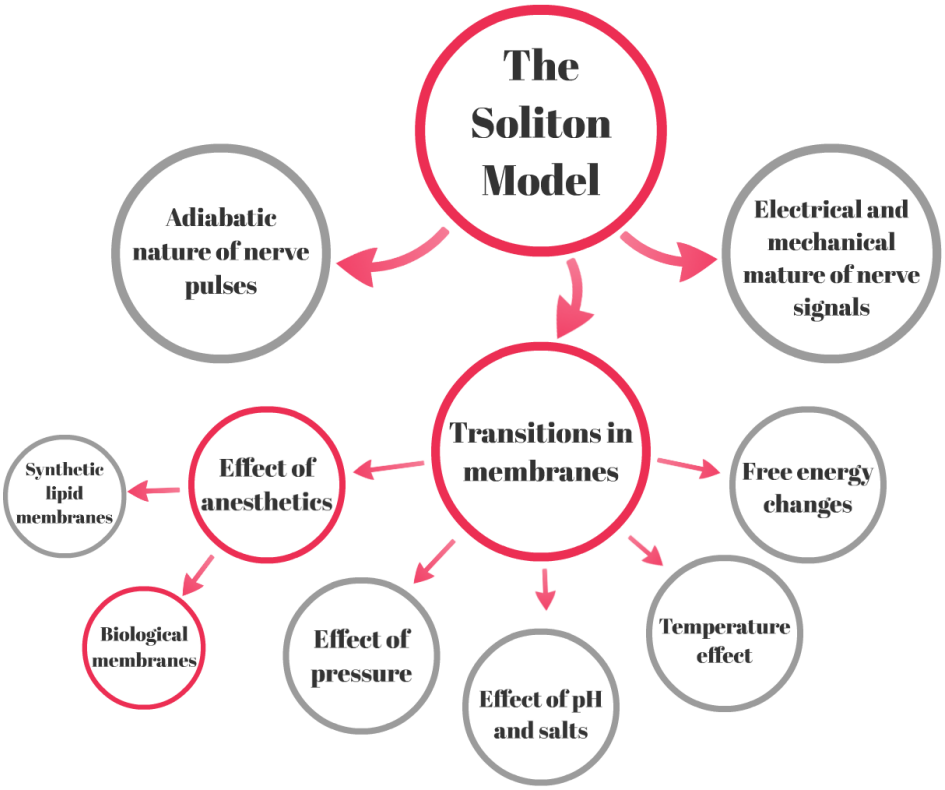

Figure 6: Schematic representation of physical aspects covered by the Soliton Model. Highlighted are some of predictions of the Model that will be addressed experimentally in this thesis.

The Model addresses the adiabatic nature of nerve pulses, the electrical and mechanical nature of nerve signals and the transitions in membranes. (Figure 6) A transition in a membrane primarily refers to the lipid melting transition which enables the propagation of solitons. The transition itself is in close proximity to the biological conditions. Any change in the membrane that influences the transition can consequently affect the propagation of a nerve signal. Anesthetics can bring about such a change. Their effect on the synthetic lipid membranes is well known [12], however no previous studies have been performed on biological samples. This thesis will experimentally address this aspect.

3 Anesthesia

3.1 Introduction

During the course of history, certain herbs, ethanol and cannabis have been known to reduce pain. At the beginning of the 19th century, the discovery of anesthetic properties of chemicals and compounds like nitrous oxide, carbon dioxide, diethyl ether, ether, chloroform and cocaine started a new era in medical treatments without pain.

Anesthesia influences all organisms to a similar degree. It can be triggered by a surprising variety of different substances, including noble gases like xenon. Although the mechanism is still not understood, the anesthetic phenomenon has been described by competing theories ascribing its effect to either lipids or to proteins.

3.2 The Meyer-Overton Rule

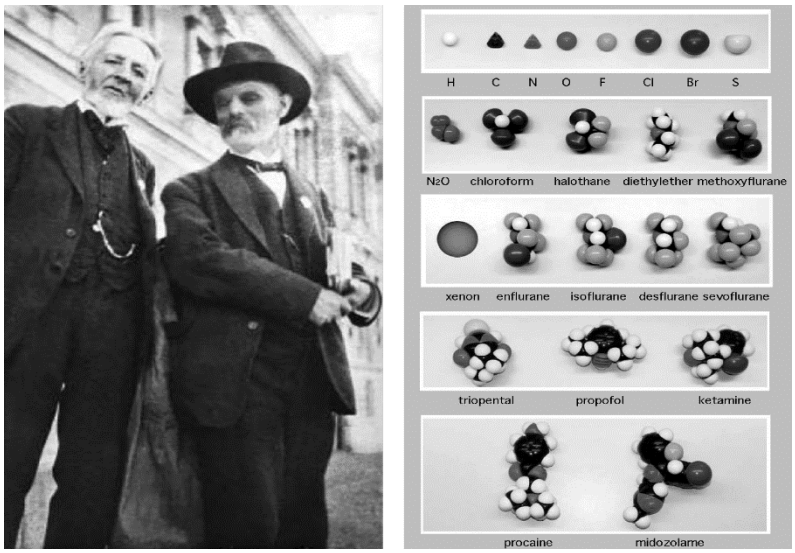

Figure 7: (Left) Hans H. Meyer and Charles E. Overton, 1910. (Right) Structure of various anesthetics. [1]

In 1901, Ernest Overton found that the anesthetic potency is proportional to the partition coefficient between water and olive oil. [13] Simultaneously with Overton, Hans Meyer came to a similar conclusion. [14]

The solubility of anesthetics in oils reflects their solubility in lipids. As anesthetics are nonreactive molecules, their potency must be a consequence of their ability to distribute in living protoplasm, more precisely, in lipids as fatty substances of membranes. The strength of the anesthetic is thus dependent on the affinity to fatty substances. All cells should be affected. However, the effect is most easily observed in nerve cells as their proper functioning results in the consciousness and the physical sensation. Furthermore, nerves have a higher composition

of lipids compared to the other cells [3] which suggests a more pronounced anesthetic effect. [14]

The Meyer-Overton rule is the empirical finding that describes the correlation between the partition coefficient P and the critical anesthetic concentration $[ED_{50}]$.

$$\frac{[C_{H_2O}]}{[C_{membrane}]} \equiv P^{-1} \propto [ED_{50}] \tag{5}$$

and

$$P \cdot ED_{50} = const. \tag{6}$$

where $[C_{H_2O}]$ is concentration of anesthetics in the water and $[C_{membrane}]$ concentration in the membrane. $[ED_{50}]$ is concentration at which half of the population is anesthetized.

By letting $[C_{H_2O}] = [ED_{50}]$, the anesthetic concentration $[C_{membrane}]$ is shown to be constant at critical anesthetic dose, independent of the chemical nature of the anesthetic drug. This means that the critical anesthetic concentration does not depend on chemical nature of the anesthetic. The same rule is obeyed by both volatile and liquid anesthetics as seen in Figure 8.

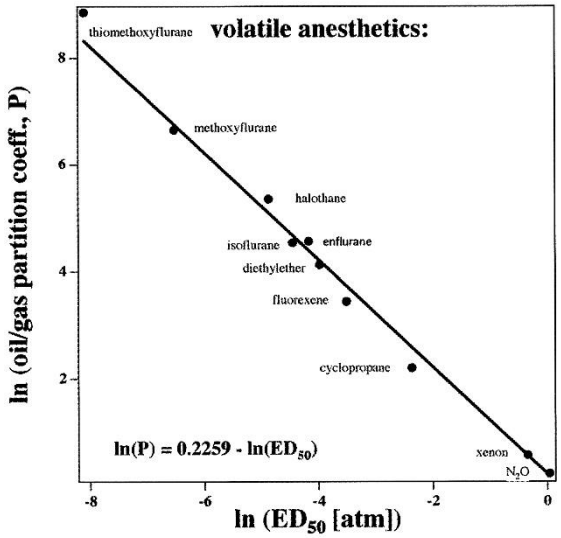

Figure 8: The Meyer - Overton correlation for volatile anesthetics [13]

The action of nonspecific narcotics depends on the fact that these compounds dissolve in brain lipids. Anesthetics change the physical state of the lipids and thus disable normal functioning of the nerve cells. This leads to the conclusion that it is likely that the brain lipids have an equal or greater role as the cell proteins in the protoplasm [13].

3.3 The Effect of Anesthetics on the Lipid Melting Points

What is the physical mechanism of anesthesia?

The mechanism of nerve pulses is closely related to the melting of lipid membranes, which can be influenced by anesthetics.

The freezing point depression effect is a consequence of the mixing entropy of anesthetics in the fluid phase. It is derived, by assuming, that when anesthetic molecules dissolve in the fluid phases of lipid membranes and do not dissolve at all in the gel phase.

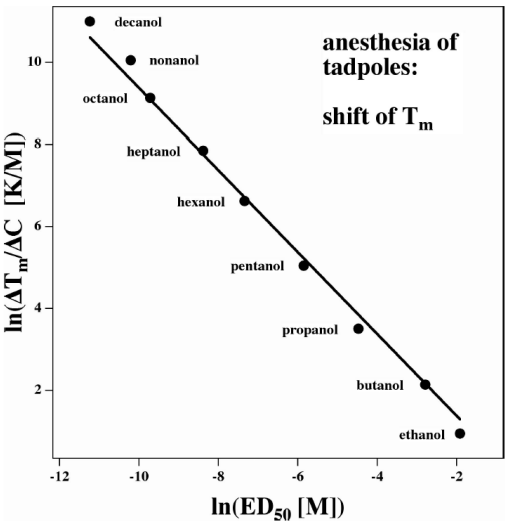

Figure 9: Concentration dependence of the melting temperature of DPPC membranes plotted against critical anesthetic dose. [1]

The freezing point depression describes the change in the melting temperature, ΔT_m , due to the presence of anesthetics

$$\Delta T_m = -\left(\frac{RT_m^2}{\Delta H}\right) \; x_A \tag{7}$$

with T_m being the melting temperature of the lipid membranes in the absence of anesthetics, x_A is the molar fraction of the anesthetics molecules in the membrane, while ΔH is the excess enthalpy of the membrane transition.

Figure 9 shows that the dependence of the melting point on the anesthetic concentration is linearly dependent on the critical anesthetic dose. [15] From the plot one obtains:

$$\ln \frac{dT_m}{dC_{anesth}} = \alpha - \ln ED_{50} \tag{8}$$

where $\alpha = -0.625$ is a constant.

If $C_{anesth} = ED_{50}$ we obtain that the shift in melting temperature at the critical anesthetic dose is $\Delta T_m = -0.53K$ independent of the drug. Likewise, independent of the drug, from data follows that the critical molar fraction of anesthetics in the membrane is $x_A = 0.026$.

3.4 Drugs used in experiments

Pentobarbital (5 - ethyl - 5 - (1 - methylbutyl) - 2, 4, 6 (1H, 3H, 5H) - pyrimidinetrione) is part of the barbiturate group, which is a large group of widely used anesthetics. At the room temperature it is a solid powder. It is commonly used both on humans and animals as a sedative, for short-term hypnosis, control of convulsions and reduction of intracranial pressure. In higher doses, pentobarbital is also a drug often used for euthanasia. Pentobarbital has been chosen because its effect on synthetic lipids has been well studied.

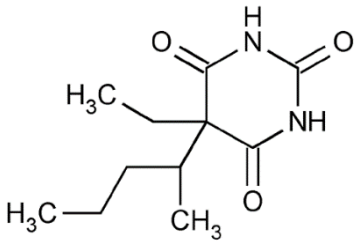

Figure 10: Pentobarbital

Flurothyl (Bis (2, 2, 2 - trifluoroethyl) ether) is a volatile liquid drug from the halogenated ether family. Unlike most of halogenated ethers which have anesthetic effects, flurothyl has opposite, stimulant and convulsing effects. It has been used for the chemical induction of seizures and in the past, as an alternative for shock therapy. By using flurothyl we wanted to investigate if the opposite effect that can be observed could be captured on the molecular level as well.

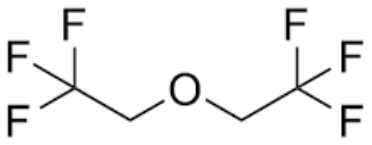

Figure 11: Flurothyl

4 Differential Scanning Calorimeter

Differential Scanning Calorimetry (DSC) measures heat changes associated with the change in conformation of molecules. It is used to characterize their physical state.

DSC directly measures the enthalpy (ΔH) and temperature (T_m) of thermally induced structural changes in biomolecules. Other thermodynamic parameters that the data provide are entropy (ΔS), Gibbs free energy and heat capacity (Δc_p)

Figure 12: Malvern's MicroCal VP-DSC in our lab (photo by Ola Jakup Joensen, NBI)

Two cells, a reference and a sample cell, are imbedded into the thermal core of the DSC that is insulated against the surroundings (Figure 13). During the experiment, the calorimeter is maintaining the same temperature of the two cells.

Both cells are heated at a pre-determined scan rate. The temperature difference between them is caused by heat absorption of the sample triggered by the conformational change of the biomolecules. DSC monitors the heat change by measuring the differential power that is supplied to the cell heaters in order to maintain zero temperature difference between the reference cell and the sample cell.

$$\Delta P = P_r - P_s \neq 0 \tag{9}$$

The difference in added heat, ΔQ can then be determined:

$$\Delta Q = \int_t^{t+\Delta t} \Delta P \; t' \; dt' \cong \; \Delta P \cdot \Delta t \tag{10}$$

where Δt is the time of the heating. Since cells are kept under constant pressure, $\Delta p = 0$, the enthalpy becomes:

$$\begin{aligned} \Delta H &= \Delta Q + V \cdot \Delta p \\ &= \Delta Q \end{aligned} \tag{11}$$

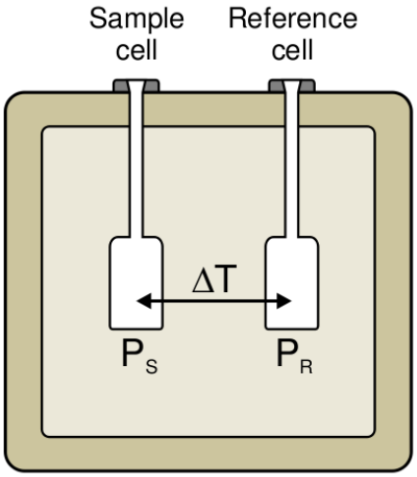

Figure 13: A schematic representation of a calorimeter. [34]

Consequently, the heat capacity, c_p, can be derived from its definition

$$c_p = \left(\frac{\partial H}{\partial T}\right)_p \cong \left(\frac{\Delta Q}{\Delta T}\right)_p = \frac{\Delta \mathrm{P}}{\frac{\Delta T}{\Delta t}} \tag{12}$$

with $\frac{\Delta T}{\Delta t}$ being the scan rate. Endothermic events are observed as positive displacements in the heat capacity. The melting temperature (T_m) is the peak value of a melting transition and the area under the curve is the enthalpy (ΔH) of the process. T_m is the temperature where both conformations of the biomolecule are present in equal amounts. In the case of lipids that would be amount of lipids in each phase, gel of fluid (Figure 3) and in case of proteins it is whether they are in folded or

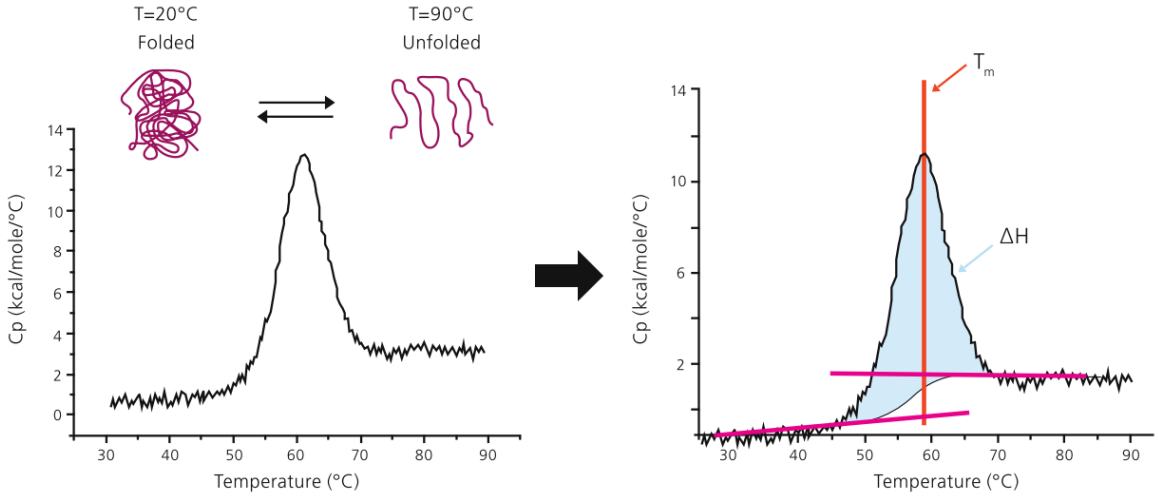

Figure 14: Example of a protein unfolding profile followed through heat changes. [16]

unfolded state (Figure 14)

Compounds that destabilize the conformation of a biomolecule will cause it to have a transition at a lower temperature and vice versa. Stabilizing or destabilizing events are either of intrinsic or extrinsic origin [16]. Intrinsic are those that occur within the molecule, like truncation or mutation of the molecule. Extrinsic factors on the other hand are external to a molecule like buffer conditions, e.g. pH, salt and ion concentrations; anesthetics etc.

5 Materials and Methods

Some biological membranes have been shown to display melting transitions somewhat below physiological temperature. However, studies on this are scarce. There is a considerable lack of studies investigating the melting properties in native biomembranes.

In this thesis project, the membranes from the spinal cord of vertebrates (sheep and pig) were investigated and the transition properties were studied in the absence and presence of drugs such as anesthetics and convulsant. A treatment and preparation of the biological samples was developed and optimized. Differential scanning calorimeter (DSC) was used to record thermal profiles of lipids and proteins in the membrane.

Three major sets of experiments were conducted. Sheep and pig spinal cord were prepared and used to demonstrate change in the heat capacity of biomembranes under constant pressure and changing temperature conditions. Simultaneously, synthetic lipid dipalmitoylphosphatidylcholine (DPPC) scans were run under the same conditions as biological ones, as a control, to observe changes in a more controlled environment.

Figure 15: Subjects of the experiments. Photograph of a sheep and a pig and an illustration of a DPPC molecular structure.

Firstly, calorimetry scans and preparation of the sheep spinal cord samples were done together with Fatma Tounsi, a MSc biochemistry student, working on her thesis in the Thomas Heimburg's Membrane Biophysics Group. She presented some of the results in her MSc thesis [17]. In preparation of the biological nerve samples for calorimetric scan, we followed some general guidelines presented in the MSc thesis [18] of a former student from our group, Søren Blok Madsen, who worked with rat brain.

Secondly, in the second part, the pig spinal cord experiments were conducted by me. Each step of the preparation process was carefully crafted to reduce the number of parameters and optimize the outcome. For future use, the pig spinal cord preparation method should be referred to as the most up-to-date version of biological samples treatment for calorimetry use.

Finally, DPPC experiments were designed to serve as a control for pig spinal cord trials by keeping some of the variables in the preparation the same. Calorimetry scans and preparation of the samples were done in collaboration with first year BSc physics students Isabella Jul Andersen, Asla Husgard, Estrid Naver, and Cecilie Toftdahl Olesen, as a part of their First year project with me being, along with Thomas Heimburg, the project supervisor. Some results were presented as a part of their project report.

Thorough descriptions of experimental setups for each of the three sets of experiments are presented below.

5.1 Sheep spinal cord

Sheep back was purchased from the local butcher shop (Alamir Halal Slagter, Tagensvej 112, 2200 København N). The animal was slaughtered by cutting the jugular vein. The meat was transported unfrozen, at low temperature from Germany. Bought back pieces were, on average, three days old at the time of purchase. When deciding on the meat quality, our conditions were that it should be relatively fresh, to avoid effects of degradation, and it should not have been frozen at any point, because that could rupture cells. A part of the animal's back was transported to the lab in an ice cooler and was processed the same day.

Figure 16: Cutting the nervous and connective tethers that exit the cord to the periphery and keep the spinal cord in place

The vertebral column was sawed and opened, exposing the cord. Peripheral nerves and tethers that exit the spine and keep it linked to the bone were cut (Figure 16). The extracted cord was then rinsed with a buffer in order to clean it from blood and bone debris. The dura mater, the membrane that envelopes the structure, was removed by cutting the cord vertically and pealing it off (Figure 17).

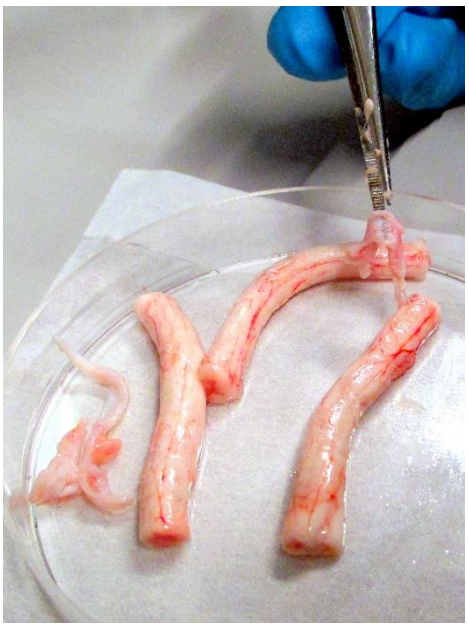

Figure 17: Extracted spinal cord with removed dura mater.

The spinal cord was then cut into smaller pieces and homogenized with a stator rotor, which yielded better results than using the pestle and mortar. The buffer was gradually added. To avoid overheating, the container was kept on ice. Process was done using rotor-stator Tissue Master 125 Watt Lab Homogenizer w/ 7 mm Probe (Omni International, Inc., Kennesaw, GA) with 30 second 33.000 RPM pulses and 30 second pauses in between over the course of 20 min (Figure 18).

Figure 18: Homogenizing the spinal cord.

The buffer used in the experiment and preparation contained 150mM NaCl, 2mM EDTA and 1mM HEPES. It was adjusted to pH of 7,42. The concentration of NaCl chosen was such as resembles one in the organism. EDTA in buffer removes the metal cofactors required for enzymes activity in the biological samples that would deteriorate the sample. HEPES is a pH buffer.

The sample was centrifuged using MSE Super Minop centrifuge (England) at 3355 RCF in 15 min intervals. After each round the supernatant was discarded, tubes were filled up to the previous level with buffer, vortexed and put in the centrifuge for another cycle until supernatant was completely clear. The majority of the fibrous tissue sediment at the bottom was removed by pouring pallet to a new tube after each round, first 2 to 3 times (Figure 19).

Several milliliters of pallet were obtained from each spinal cord.

Pentobarbital was used as an anesthetic. A 10mM stock solution of pentobarbital (Sigma-Aldrich, St. Louis, MO) in methanol was made and distributed in the required quantities to empty flasks. It was then dried under air stream and high vacuum for 3 hours. Sheep spinal cord samples were added to the flasks, mixed and vortexed until no visual residue of the drug was seen on the sides. Samples were degassed before proceeding to the filling the calorimeter.

Figure 19: Centrifugation of the sample in MSE Super Minop centrifuge. (photo by Ola Jakup Joensen, NBI)

Flurothyl (Sigma-Aldrich, St. Louis, MO) was used as a convulsant. Since it is fluid at room temperature it was added to the sample using a transferpettor. Also, since it is volatile, samples were degassed before being introduced to the drug.

The calorimetry cells were carefully filled to avoid air bubbles (Figure 20). The buffer was used as a reference. Scans were run within the standard working range of the VP-DSC calorimeter (MicroCal, Northampton, MA) from 1 to 85 °C at the 40 deg/h rate.

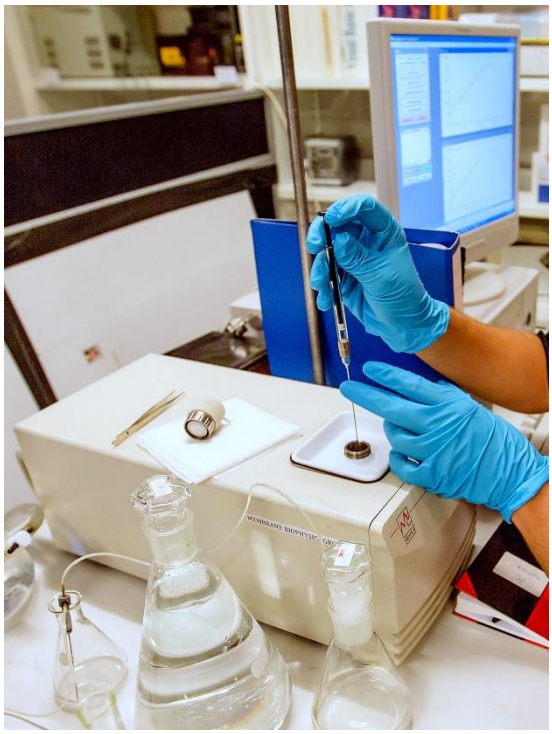

Figure 20: Filling the VP-DSC (photo by Ola Jakup Joensen, NBI)

Several chemicals were tested for thorough cleaning of the calorimeter, which was required after each scan, since denatured proteins have a tendency to stick to the surfaces. Aqueous solution of HCl >30% yielded the best results. Cells were cleaned with 1% mucasol detergent (Sigma-Aldrich, St. Louis, MO), water and then soaked for 1 hour at 40°C in HCl. Upon removal of the acid, calorimeter was profusely cleaned with water. To test cleanliness of the cells, buffer – buffer baseline scans were performed before each sample scan.

5.2 Pig spinal cord

INTRODUCTION AND MOTIVATION

There have been a couple of ideas for improvement that arose from the study of the sheep spinal cord. Repeatability of the experiments might be upgraded by improving condition of the meat, eliminating sediment of larger fibrils, optimizing cleaning procedure and expanding temperature range of the DSC scans.

In order to optimize the procedure, each step was carefully thought through. What follows is a detailed step-by-step description of the procedure, accompanied with the arguments and motivations for each decision made along the way.

SPINAL CORD SOURCE AND CONDITION

In order to minimize transportation time and potentially varying conditions under which the meat can be found, a survey of potential suppliers was done. Contacted veterinary departments and hospitals linked to Copenhagen University all use a mixture of pentobarbital and other sedatives to euthanize animals. Cases where animals are stunned using non-chemical methods and exsanguinated are rare. This would restrict the flexibility of timing the experiments.

Another option would was getting in contact with one of the four slaughterhouses in the Greater Copenhagen region listed by the Ministry of Food, Agriculture and Fisheries, Danish Veterinary and Food Administration [19]. However, due to their remote location I have not approached them.

The pig spinal cord was purchased from the local butcher shop, which receives deliveries on regular basis from local slaughterhouses (A/S Slagteren Ved Kultorvet, Frederiksborggade 4, 1360 København K). The pig spinal cord has been chosen over sheep because of practical reasons. Since there is a higher demand for this type of meat, it is delivered on a weekly basis. Due to difference in animal size, more samples can be extracted from a pig.

At the time of the purchase the spinal cord and part of a backbone were about a week old. During that time, it was kept on low but not freezing temperatures.

SPINAL CORD EXTRACTION

The greater part of the cord was removed from the surrounding bones by the butcher and remaining parts by me. One way to reach the cord itself is to cut the bones with a saw at their thinnest point, which is located on each side of the bone of vertebra's bulge (Figure 21). After removing the body of vertebra, tethers that keep the cord linked to the body of vertebra were cut. The dura mater and the arachnoid, the outer and the middle layer of the cord itself were cut following the direction of the cord and pealed from it using a pair of scissors and tweezers. Beneath was another membrane, the pia mater, which could be easily distinguished as it is full of veins and capillaries. At the places where the pia mater was ruptured, gray and white matter of the spine was pouring out (Figure 22). It was collected in a beaker upon squeezing the structure. Approximately 13 ml of matter was collected.

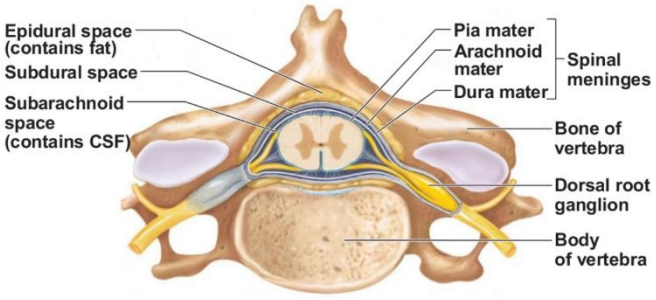

Figure 21: Cross section of spinal cord and vertebra. [35]

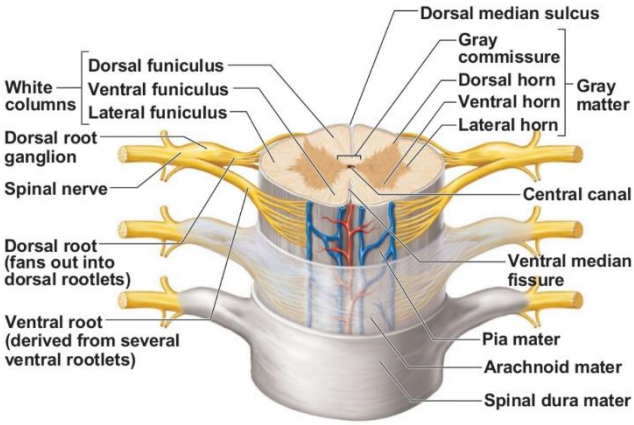

Figure 22: The spinal cord and its meningeal coverings. [35]

BUFFER

The phosphate buffer used for the preparation of the sample and later for calorimetry scans contained 150mM NaCl, 10mM Na_2HPO_4 and 1,8mM KH_2PO_4; the pH was adjusted to 7,40 with titrinorm error of ±0,02 using 1M NaOH and 1M HCl. The buffer was autoclaved with Systec type DB-45 (Systec GmbH, Wettenberg, Germany) on the liquid cycle at 121°C and pressure of just about 230kPa. Buffer was stored on the room temperature.

Due to the initial considerations to use collagenase for the treatment of the collagen, the insoluble fibrous protein in the extracellular matrix, the typically used buffer would not be suitable since EDTA inactivates the collagenase. Moreover, phosphate based buffers have lower heat contribution on the calorimetry profile [20]. Furthermore, common biological buffers such as TRIS and HEPES are not recommended for

calorimetry due to their high heats of ionization. [21] That is why phosphate buffered saline is normally used in experiments with biological samples where signal is low and effect of the buffer baseline could considerably affect the data. Collagenase ended up not being used.

In addition, Sodium phosphate buffer does not exhibit a pH shift as a function of temperature [22]. For biological research, phosphate-buffered saline (PBS) is commonly used. The most common recipe contains 130mM NaCl, 2,7mM KCl, 10mM Na_2HPO_4 and 1,8mM KH_2PO_4. The molarity of NaCl was kept from the previous buffer as it closely resembles salt concentration in the body [23] and KCl was removed to reduce the number of parameters. The pH was chosen to match the approximate pH of the blood of a pig which is in the range 7,35 - 7,45 [24].

HOMOGENIZATION

The spinal cord was homogenized on 33.000 RPM in 30 second pulses with 30 second breaks between them during a 30 minute period using a rotor-stator Tissue Master 125 Watt Lab Homogenizer w/ 7 mm Probe (Omni International, Inc., Kennesaw, GA). Buffer was gradually added to the sample. To make sure that protein denaturation due to heat production does not occur, the flask with the sample was kept in an ice bath and homogenization was conducted in intervals. Roughly double the weight of initial sample was added in buffer along the process. The process was completed when no visual clumps could be observed in the structure. [25]

FILTERING

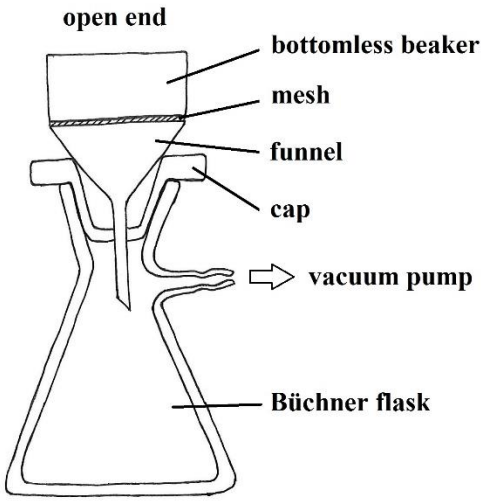

Figure 23: Filtering setup outline

The homogenized sample was filtrated through stainless steel, 100 mesh with 140µm opening size (Ted Pella, Inc., Redding, CA) using a self-designed and constructed apparatus depicted on Figure 23. An improvised Büchner funnel made out of a bottomless beaker, mesh and funnel were glued together and attached to the flask through a cap with a hole in the middle. The hose barb of the Büchner flask was connected via vacuum hose to a vacuum pump. After the vacuum pump has been turned on, pressure pulled the sample through the mesh into the beaker. A mesh profile of 140µm opening size was chosen to filter out larger fibrils [26].

At this point, the sample contained ca. 13g of spinal cord tissue and about 50 ml of buffer that was added during the process. After filtration, the sample was collected and distributed in centrifuging flasks. Since the pelleting capabilities of the centrifuges we own in the lab are different the sample was divided in two. Half of it was centrifuged in MSE and half in Eppendorf centrifuge. Finally, the supernatant from MSE centrifuge was attempted to pellet in the Eppendorf centrifuge.

First half, two times 14 ml of the mixture were centrifuged in MSE Super Minop centrifuge (England) in 15min intervals at 3355 RCF, which corresponds to the 4400 RPM at this centrifuge. After each round the supernatant was removed and the pellet was mixed and vortexed with newly added buffer that has been filled up to the previous level of the mixture. The process was repeated until the supernatant was completely clear. This took, in this case, nine centrifuging intervals. The final pellet of about 3,5 ml was stored in the fridge.

Second half, fifteen 1,5ml of mixture was processed in the Eppendorf centrifuge (Hamburg, Germany). Samples were run at 20800 RCF for 10 min. Supernatant was discarded and replaced with buffer. Each flask was thoroughly mixed and vortexed until the entire pallet was dissolved in newly added buffer. This procedure was repeated for five times. It resulted in ca. 700 µl of pallet in each of the flasks. In order to remove samples from tubes more easily and later, have a manageable thickness for calorimetry use; each pallet was mixed with 500 µl of buffer, vortexed and finally stored in the fridge under name P1ES (Pig 1 Eppendorf Sample).

Finally, the supernatant from MSE centrifuge was distributed to eight 14ml flasks and run for two times for 15 min in the centrifuge on 3355 RCF. Supernatant of the supernatant was distributed in 30 - 1,5ml flasks and centrifuged at 20800 RCF for 15 min in the Eppendorf centrifuge. Because of its small volume and thickness, pelleted sample was not further used. It would have been hard to produce a homogeneous sample that could be used for the calorimetry scan.

Parameters	Low speed	High speed	Ultracentrifuge
Speed ranges (r.p.m. x 10^3)	2–6	18–22	35–120
Maximum RCF (x 10^3)	8	60	700
Pelleting Applications			
Bacteria	-	Yes	Yes*
Animal and plant cells	Yes	Yes	Yes*
Nuclei	Yes	Yes	Yes*
Precipitates	Some	Most	Yes*
Membrane organelles	Some	Yes	Yes
Membrane fractions	Some	Some	Yes
Ribosomes/polysomes	-	-	Yes
Macromolecules	-	-	Yes
Viruses	-	Most	Yes

* Can be done but not usually used for this purpose

Figure 24: Classes of centrifuges and their applications. [36]

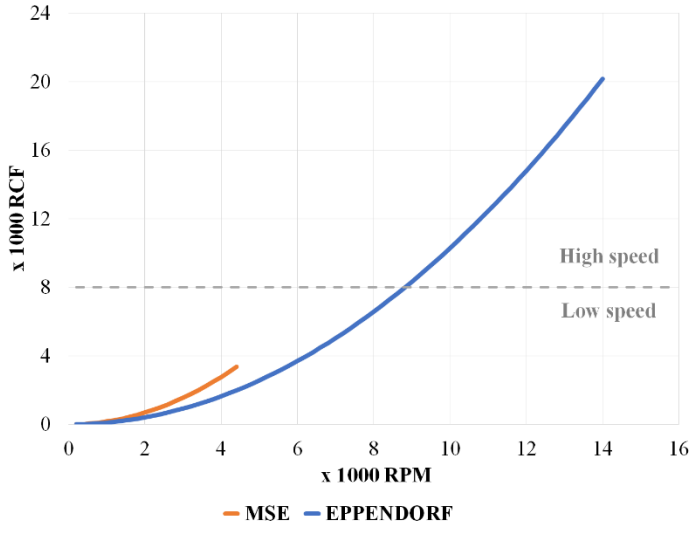

Figure 25: Maximum revolutions per minute (RPM) of a centrifuge with calculated corresponding relative centrifugal force (RCF) values, for MSE and Eppendorf centrifuges in our labs.

The main motivation for the use of the Eppendorf centrifuge, in this round of experiments (pig spinal cord), was to ensure that the membrane parts were pelleted which might not be the case for the MSE centrifuge speed range (Figure 25). As seen in the table in Figure 24 and, high sped centrifuges with 18000 to 22000 RPM have a pelleting application for membrane organelles and fractions (as well as other heavier fractions of the biological sample).

PREPARATION OF THE SAMPLE FOR A DSC SCAN AND SCAN SETTINGS

To avoid freezing of the content of the cells and thus damaging the apparatus, glycerol was introduced to lower freezing point of the sample. For easier calculation, the sample was assumed to have the same freezing point as water. 30 wt. % of glycerol in water brings down freezing point by 9,5°C and increases the boiling point to 103°C [27]. In addition to glycerol, the buffer used contained salts that would also contribute to the freezing point depression. The reason to do so was the fact that the beginning of the phase transition in sheep spinal cord samples was not clearly visible in scans produced in the standard working range of the calorimeter which is from 1 to 90 °C.

30 wt. % of glycerol (of 95% purity) in buffer was recorded as a baseline for further experiments. The profile accounts for manufacturing differences between measuring cells.

Two scans were run for each concentration of anesthetic. 2ml of sample were prepared for each pair of scans. A stock solution of pentobarbital was made in ethanol. The required amount would be added into a sample flask, dried under an air stream, and put under high vacuum for 3 hours. 2ml of spinal cord sample were added to the dried anesthetic. In order to dissolve, the sample was vortexed and mixed until no visual residue of anesthetic was seen on the sides of flasks. 30 wt. % of glycerol 95% was introduced to the mixture. After vortexing the sample and the buffer, which contained the same amount of glycerol as the sample, the samples were degassed for

10 min or put for a short pulse on gas ballast mode under high vacuum until bubbles were sucked out.

Before filling the calorimetry cells, remaining water from the cleaning was removed and cells were rinsed with buffer containing glycerol. Buffer with glycerol was used as a reference. Both cells were filled in a pulsatile manner in order to push out all potential bubbles.

Each scan was run on 0,5152ml of the sample (which is the size of the calorimeter cell) which contained around 40 to 50 mg of dry matter. The weight of dry substance was measured by drying the sample under air stream and high vacuum.

The preparation of the spinal cord for the calorimetry scan took one week due to time needed for construction of filtering parts. At the point of the first scan the sample was 2 weeks old counted from the day the animal was slaughtered.

The measurement of the excess heat capacity as a function of temperature was performed on a Microcal differential scanning calorimeter, VP-DSC (MicroCal, Northampton, MA). Heating rates were kept at 20 deg/hour, the filtering period was 5 seconds and feedback was set to none. As it was found out during sheep spinal cord experiments, this rate obtained the least noise. The feedback mode was disabled because sharp transitions were not expected. In the beginning of all of three consecutive up-scans the sample was termostated for 15min at starting temperature. Scans were run from -8 to 100 °C.

No signal averaging or other forms of data smoothing were applied to the thermograms. The data was processed using IgorPro.

CALORIMETER CLEANING PROCEDURE

After the scanning procedure was completed, both reference and sample cell were emptied and generously rinsed with water until water in the syringe became completely clear. Cells were then rinsed with 37% hydrochloric acid once, and then filled and left for 1h to thermostat at 50°C. While thermosetting, the opening of the calorimeter was covered with dampened tissues instead of the original cap to prevent damage. During this process safety goggles, gas mask, lab coat and gloves were used to minimize exposure. After removing the acid from both cells, pressure sensor hole and outer, visible parts of the calorimetry opening were generously rinsed with water and then ethanol to prevent any HCl residue that evaporated during the thermostatting time to later contaminate the sample in the cells. Gas nitrogen was used to completely dry all the parts. Up until now, only syringe was used for cleaning. Each cell was then washed using cleaning system for 5min with 1% mucasol - the detergent (Sigma-Aldrich, St. Louis, MO), 5 min with ethanol and 30min with water, which

would correspond to 33ml of mucacol and ethanol and 200ml of water. As for the syringe, it was rinsed with water straight after being in the contact with the acid, and in the end washed with ethanol and then water, and finally dried with gas nitrogen.

This cleaning procedure takes around 3h to complete.

Calorimetry manual was consulted in order to choose the chemical that could be suitable for thorough cleaning and would not, at the same time, damage the titanium cells. Since denatured proteins have a tendency to adhere to the surfaces, hydrochloric acid was left in the cells for longer time and on higher temperature to improve effectiveness.

Thorough cleaning of outer parts of the calorimetry opening was performed since HCl evaporates from cells and contaminates outer parts during the thermosetting. If left unwashed, the pH of the sample could be altered and consequently results would be compromised. These could be observed as brown droplets on the visible parts of the opening after the scan of the biological sample is completed.

Both cells and syringe finally are to be cleaned with at water to prevent eventual residue of ethanol to come in contact with the sample and potentially alter the profile as it is an anesthetic.

LIPID EXTRACTION

Lipids were extracted from the pig spinal cord sample following the Bligh and Dyer method. [28]

To a 1ml of sample, 3,75 ml of a mixture of chloroform/methanol (1/2) was added. The mixture was vortexed for 10 min. After adding 1,25 ml of chloroform and mixing for 1 min, 1,25 ml of water was inserted, mixed and vortexed for 3 more minutes. The mixture was centrifuged at 2773 RCF which corresponds to 4000 RPM for the MSE Super Minop centrifuge (England) for 13 min. As seen in Figure 26 two phases and a protein disk in the middle could easily be distinguished. It was left for half an hour to settle down because immediately after centrifugation the lower phase got misty while the upper remained clear. Later, the lower phase started to get clearer and upper dimmed. The reason could be that the centrifuge speed

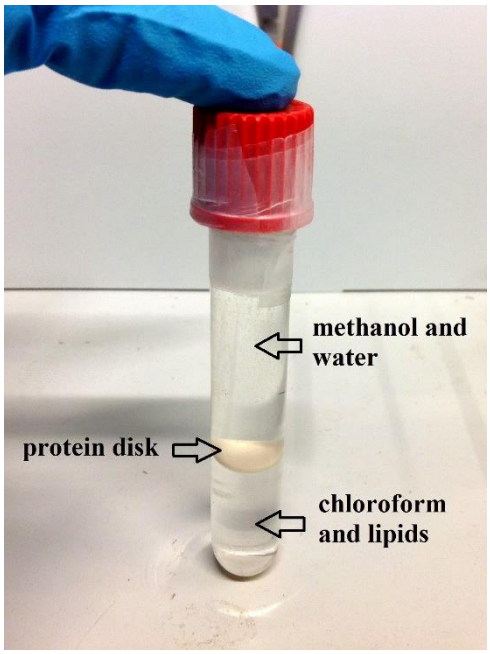

Figure 26: Bligh and Dyer lipid extraction method

was too high, pushing the proteins from the protein disk in the lower phase. In the literature and websites describing the method, there is no reference to the proposed centrifuge speed, to my knowledge.

The lower phase was collected in a glass bottle. While penetrating upper phase and protein disk bubbles of air were released from the syringe in order to avoid contamination of the with upper layer.

Lower phase with lipids was dried overnight under the air stream and then placed in Trivac B vacuum pump (Oerlikon Leybold Vacuum, Cologne, Germany) for 4 hours at about 10^{-4} mbar.

0,0797g of lipid was obtained. Dried lipids were stored in the fridge for 39 days before they were further processed for the calorimetry scan.

Throughout the process of extraction, glass utensils, pipettes and syringes were used in order to prevent chloroform degradation of the plastic.

PREPARATION OF EXTRACTED LIPIDS FOR CALORIMETRY SCAN

After removing them from the fridge, lipids were put in the vacuum chamber for 1h. 2ml of phosphate buffer was added to dried lipids. Sample was mixed, vortexed and heated in the water bath up to 95°C, until it could be seen that the majority of the lipids were dissolved. Sample was degassed for 15 min before it was put into the calorimeter.

The rest of the sample was stored in the fridge for 10 days before it was used. After reaching room temperature, it was vortexed and mixed again and this time it could be seen that all the lipids were dissolved in the buffer. Forthwith, the sample was degassed in vacuum chamber on gas ballast mode under lower pressure, for a short pulse, until it could be seen that the bubbles were sucked out of the sample.

SCAN SETTINGS

The sample was scanned in the standard working region of calorimeter, from 1 to 90°C, with a filtering period of 5 seconds and 15 min of thermosetting before each scan. The first scan was run to set the lipids to the same thermal history with scan rate of 40 deg/hour and no feedback while second one was done at a slower rate of 5 deg/hour and high feedback, the usual settings for lipid samples.

5.3 DPPC

Dipalmitoyl phosphatidylcholine (DPPC, Avanti Polar Lipids, Birmingham, AL) was used without further purification. DPPC was kept at -20 °C. To prevent the lipids from absorbing water from the air and consequently changing molecular mass and degrading through the process of hydrolysis, the container was thawed and set to reach room temperature before use. Ten samples of 10mM concentration were prepared in chloroform. Samples were than dried out under air stream and under high vacuum for 3 hours. In between treatments, flasks with DPPC were kept in the freezer.

A stock solution of pentobarbital (Sigma-Aldrich, St. Louis, MO) in ethanol was made and added to dried DPPC samples in required amounts (1mM, 2mM, 4mM and 8mM). The mixture would then be dried out again, under the air stream and for 3 hours in high vacuum. Pentobarbital is solid and has a melting point of 130°C [27] which makes it unlikable to evaporate.

In order to replicate conditions as in pig spinal cord samples, phosphate buffer of the same content was used. It contained 150mM NaCl, 10mM Na_2HPO_4 and 1,8mM KH_2PO_4. The pH-value was set to 7,4 and buffer was sterilized in an autoclave on liquid cycle (121°C and ca. 230kPa).

Prepared DPPC and pentobarbital were dissolved in phosphate buffer by vortexing and heating in a water bath at a temperature above the phase transition, until no visible clumps remained (>75°C and for >30 min).

Lipids were not extruded, which means that experiments were done working with multi-lamellar vesicles (MLV) where membrane layers are stacked one on top of one another forming 1 – 10 µm structures. The transitions of MLV's are highly cooperative, meaning that lipids have a tendency to be in the same phase. This produces a sharp transition in calorimetry scans.

For the scans that are out of standard working temperature range of the calorimeter (1° - 90°C), 30 wt. % of sample was added in glycerol to prevent freezing and consequently damaging cells. 30 wt. % of glycerol in mixture decreases the melting point of water to -9,5°C and it also increases the boiling point to 103°C. [29] Mixed and vortexed sample was than degassed for 10 min. Both DSC cells were rinsed with buffer glycerol mixture before proceeding to filling. Phosphate buffer with 30% wt. glycerol was used for the reference cell. Calorimetric cells were filled in pulsatile

manner to avoid bubbles. Two scans were run for each sample. Cells were thermostated at starting temperature for 15 min before each scan. The first scan was fast, 40 deg/hour rate hysteresis scan. The second scan, which was used for analysis, was a 5 deg/hour scan with filtering period of 5 seconds and high feedback since sharp transitions were expected.

6 Results and Discussion

6.1 Calorimetry Data

This chapter will present the data acquired by differential scanning calorimetry experiments. Similarly to the Materials and Methods chapter, it is divided in three sections which correspond to three groups of experiments; the sheep spinal cord, the pig spinal cord and DPPC measurements.

Due to the different amount of data obtained from sheep and pig spinal cord experiments, a different nomenclature has been used to classify graphs.

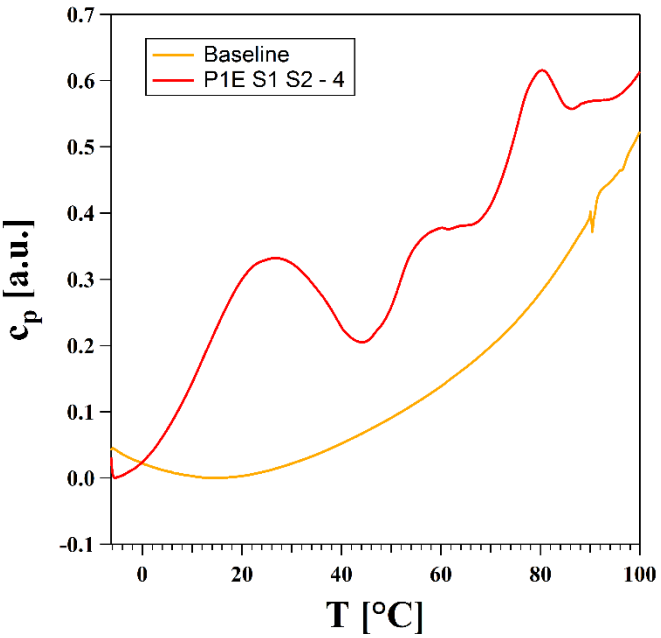

Figure 27: "Buffer" baseline (orange) and a raw data from a pig spinal cord heath capacity profile (red).

There have been 5 individual sheep spines that have been processed. Presented here are results from spine no.4 and no.5. Each cord gave enough material for a couple of scans that have been exposed to different chemicals.

For the pig spinal cord, the presented experiment results come from one spine. The extracted volume has been enough to prepare 5 samples. Each sample had enough material to run 2 scans (insert the sample in the calorimeter, run it, remove it, refill it with the second half of the sample and run it again). Each scan produced multiple profiles in different temperature ranges. One of the samples was run three times in -8° to 100°C range and the other would have three pre-scans in the region from 1° to 43°C followed by three full -8° to 100°C scans. E.g. in Figure 27, P1E S1 S2 - 4 means Pig 1 (Eppendorf centrifuge) Sample 1 Scan 2 - profile 4. This naming classification of each profile does not contain the conditions of the sample. They will be explicitly stated next to the name in each graph. This nomenclature has been used for pig spinal cord only.

The presented heat capacity profiles are not raw data. The data have been processed using the Igor Pro 6.37 (©1988-2014 WaveMetrics, Inc. Oregon, USA).

The “buffer” baseline which accounts for the manufacturing differences of the measuring DSC cells has been deducted from each heat capacity profile. Unlike synthetic lipid profiles where the baseline effect is relatively negligible compared to the heat capacity and can be removed by polynomial fit, here this effect had to be taken into account as it has comparable magnitude to the broad transitions of sample profile itself (Figure 27).

Moreover, the heat capacity in the units of $J/mol \cdot K$ is used for the profiles of synthetic lipids, like DPPC where molar concentration of the lipid sample is known. In the complex case of biological samples, it is hard to know the exact composition of the sample especially because it contains proteins alongside different species of lipids. That is why for the biological samples, sheep and pig spinal cord, the unit of $J/g \cdot K$ has been used. Weight in grams represents the dry weight of a measured sample. The units have been set to arbitrary units [a.u.] in the cases where we did not perform the weighing of the dried out sample.

Furthermore, it should be noted that the calorimeter records the absolute change in heat capacity with the starting point of the recording being usually negative value as it compares it to the heat capacity of the water. Deviation in density of the material being scanned thus changes the “starting” point of the recorded profile as well as the amplitude. Y-axes offset adjustment has been performed in most of the scans to enable a meaningful comparison between them. In scans where offset (y-axes shift) has been changed it will be explicitly stated. E.g. in Figure 27 the zero of heat capacity has been set to the lowest points of both graphs.

Additionally, when determining the peak values of the transitions, a polynomial fit of the curves was performed. Calculated maxima from the fitted curve are presented without error bars.

6.2 Sheep spinal cord

The majority of the scans were run two times for each sample. Comparing those two gives us an insight about reversible and irreversible processes that occur in the sample. The samples contain lipids and proteins. Lipids undergo phase transition, from gel phase at lower temperatures to fluid phase at higher. This process is reversible. Proteins are known to denature at high temperatures.

Figure 28 shows the comparison of the first and second scan of the same sample. In the first scan proteins unfold and in the second the lipid peak become more pronounced. This has been observed in every sample. The reason for the change in the amplitude of the lipid peak could be that more lipids undergo the transition once that denatured proteins are not imbedded/bound to the lipid membrane.

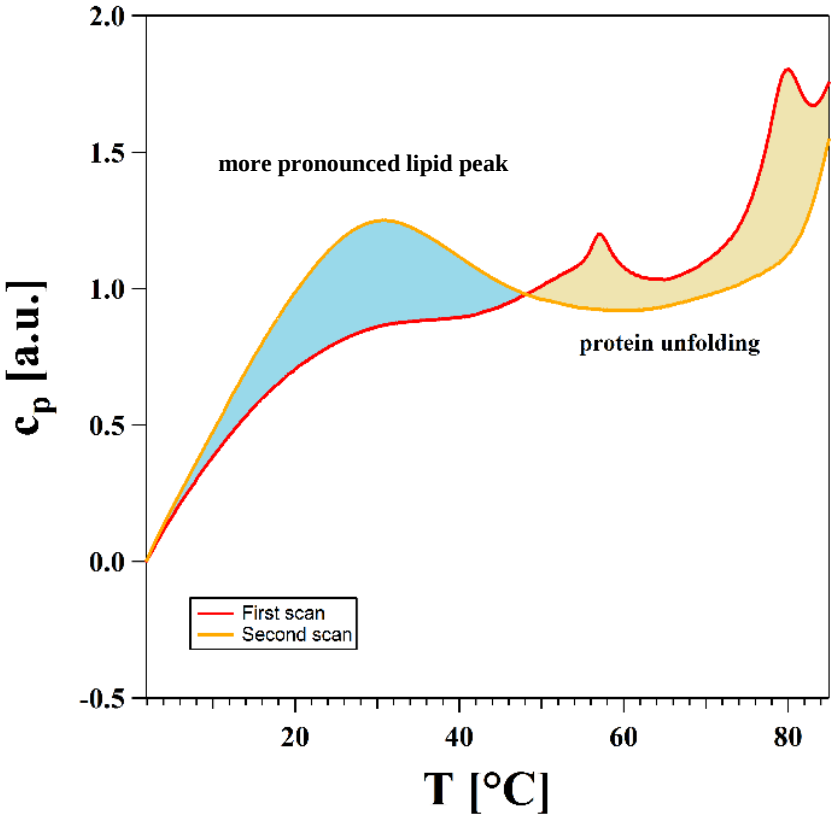

Figure 28: Sheep spinal cord no.4. The sample has been scanned two times. After the proteins denature the lipid peak becomes more pronounced. (offset: zero at the beginning of the scans)

6.2.1. Pentobarbital and Flurothyl

In Figure 29 it can be seen how drugs have an effect on the heat capacity profile. Although expected primarily in the lipid region, a shift can also be observed in the protein denaturation part of the scan. Both pentobarbital (anesthetic) and flurothyl (a convulsant) lower the temperature at which proteins denature. This is an interesting finding. Firstly, the fact that anesthesia is caused by a large variety of different molecules including noble gases (inert gases) speaks against mechanisms based on the binding of anesthetics to proteins [1]. Contrary to this, in Figure 29 it could be seen that anesthetics affect the thermodynamical properties of the proteins as well as lipids. Secondly, since the convulsants have a stimulative effect, which is opposite to that of an anesthetic, we assumed that the drug will have an opposite effect on the transition as well. Shifting the membrane to a gel state at the physiological temperature. Although, the graphs do not clearly show the effect flurothyl has on the lipids, the protein denaturation temperature peak shifts in the same manner as the one in the presence of anesthetics.

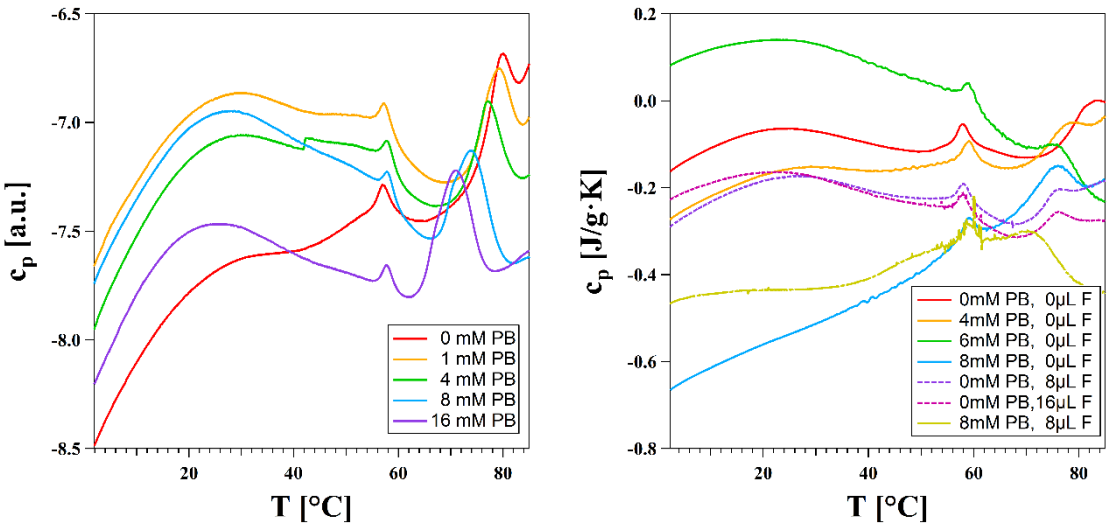

Figure 29: First scan of samples introduced to the different amounts of pentobarbital (PB) and flurothyl (F). Sheep spinal cord no.4 (left) and no.5 (right). Both pentobarbital and flurothyl produce shift in the profile. The most pronounced effect could be seen in the region attributed to the protein denaturation. Both drugs have the same qualitative effect on the profile. (offset: no offset adjustment (left) and equidistant offset between protein peaks (right))

With protein denaturation occurring at high temperatures, in the second scan we lose that part of the information. When adding anesthetic at the room temperature, they might not be dissolved as they would at higher temperatures, because below the transition lipids are in the gel phase in which anesthetics do not dissolve or do not dissolve ideally. After the sample goes through the whole temperature range the anesthetics dissolve in the fluid phase of the lipids and the sample reaches thermal

equilibrium. The lipid phase transition occurs at physiologically relevant temperatures, contrary to protein unfolding. That is why further analysis will be performed on the second scans.

As seen in Figure 30, pentobarbital lowers the melting point of the lipids. In Figure 31 peak points are plotted against the pentobarbital concentration in the samples. All data points obey nonlinear trend.

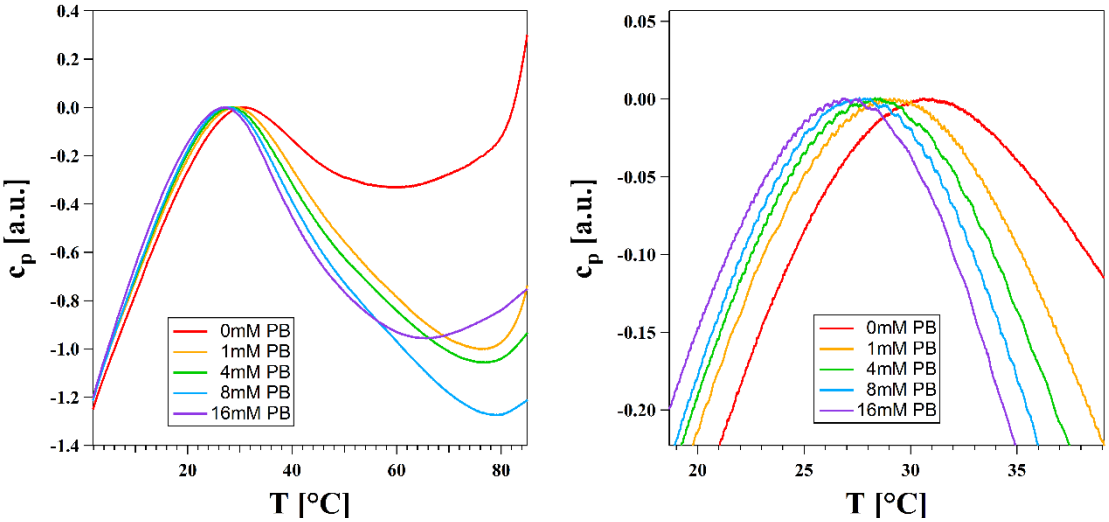

Figure 30: Second scans of sheep spinal cord no.4 samples introduced to the different amounts of pentobarbital. Full profile (left) and zoom in on the same graph (right). (offset: zero at the lipic peaks)

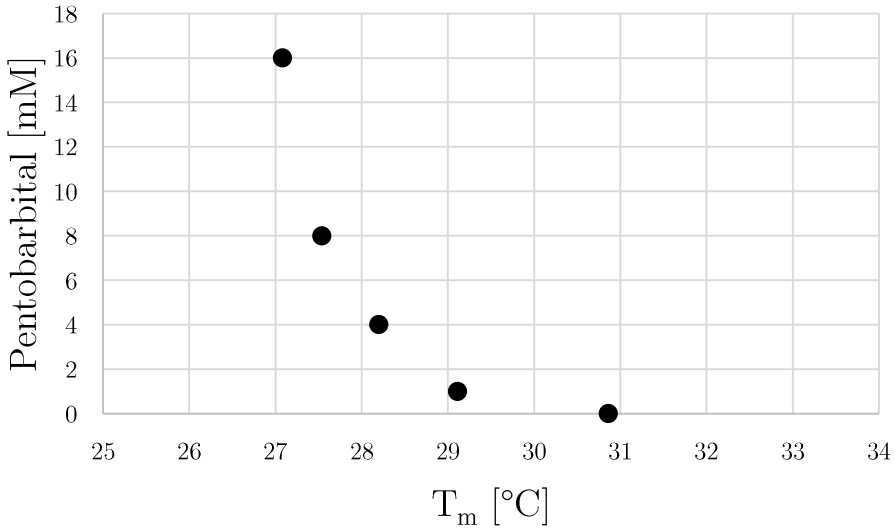

Figure 31: Melting temperature value (peak value) of the each sample was plotted against the amount of mM of the pentobarbital in the sample. Pentobarbital decreases the melting transition of the lipids in the sample. It should be noted that independent variable on the graph is temperature. The axes have been switched for easier comparison with the scan profiles.

6.3 Pig spinal cord

Similarly to the results of sheep spinal cord, we can observe two main changes that appear after a full temperature range scan has been performed (Figure 32). The first of them is the irreversible protein denaturation and the second is a more pronounced lipid peak in the following scan. The experimental proof for identifying that part of the profile to the lipids will be discussed later in this section. In the pig spinal cord experiments, one more transition peak can be observed around the body temperature of the animal (marked with an arrow). The transition "disappears" in the following scans, an observation lead to the conclusion that the transition is due to protein denaturation. However, such an explanation is unlikely due to its proximity to the physiological temperature. The possibility of the transition being spinal cord specific cannot be ruled out.

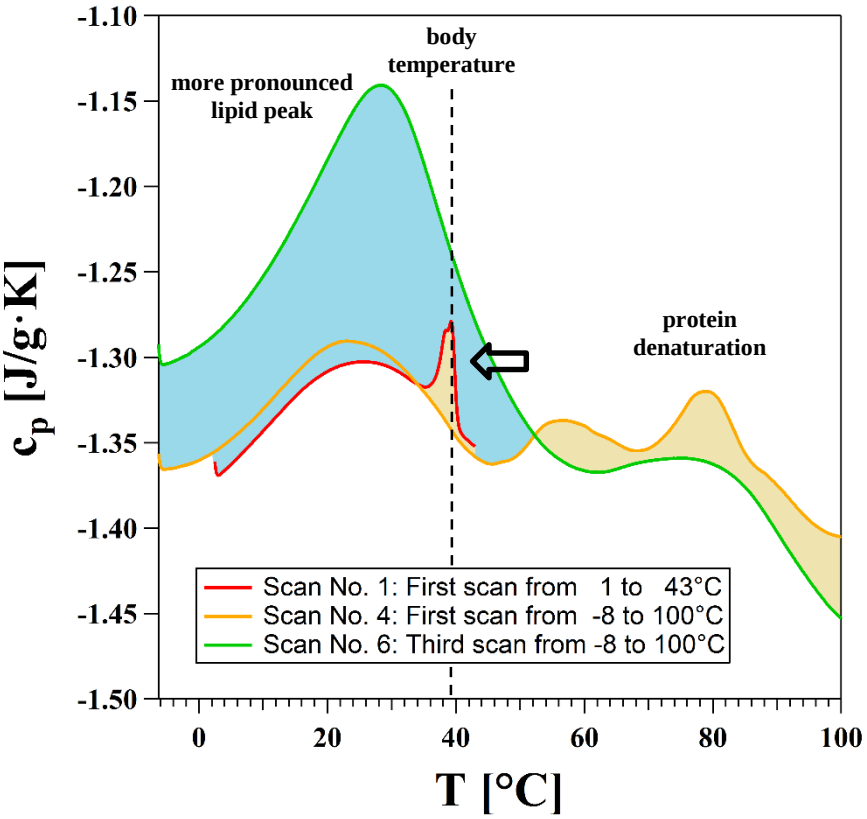

Figure 32: Pig spinal cord scans. First scan (red), apart from the broad lipid peak, it shows a sharp transition at around body temperature of the animal. The sharp peak disappears in following scans. The first scan of the whole temperature range (orange) shows protein unfolding and aggregation. Final scan (green) has more pronounced lipid peak. (offset: zero at the end of the lipid transition)

6.3.1. Pentobarbital

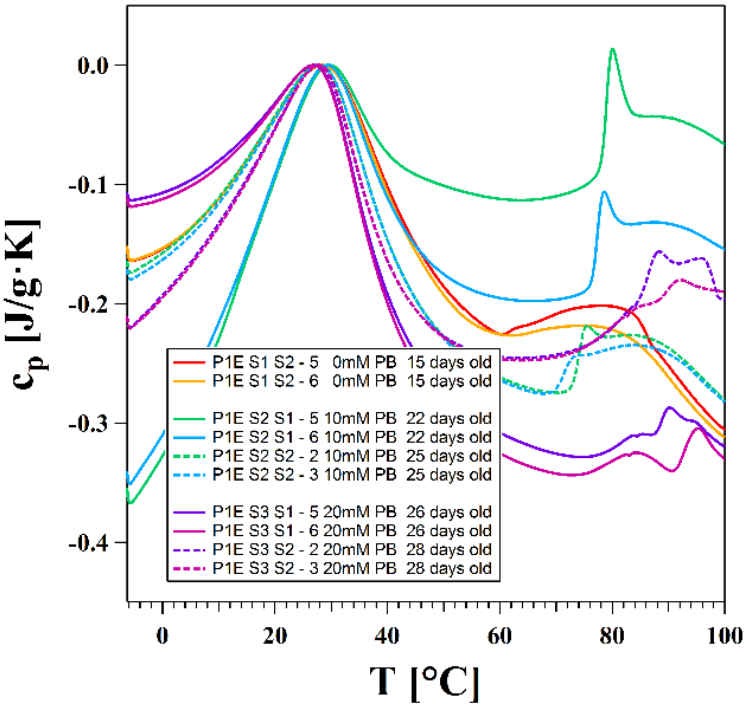

Figure 33: Second and third full temperature range scans of pig spinal cord exposed to different amounts of pentobarbital. Three samples, each with different amount of pentobarbital, were each scanned two times which produced four profiles for each sample (two for each scan). (offset: zero at the lipid peaks`

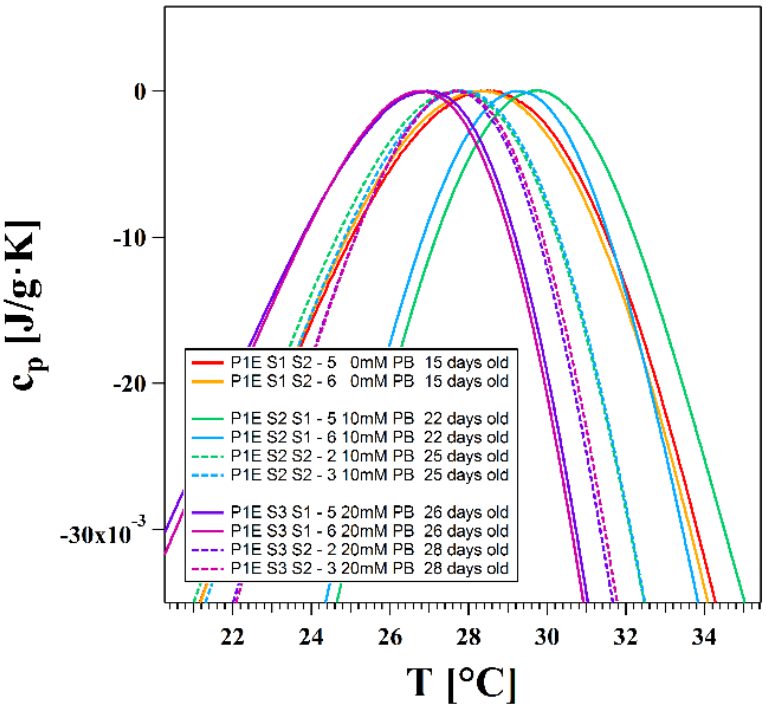

Figure 34: Zoom onto main transition of a Figure 33

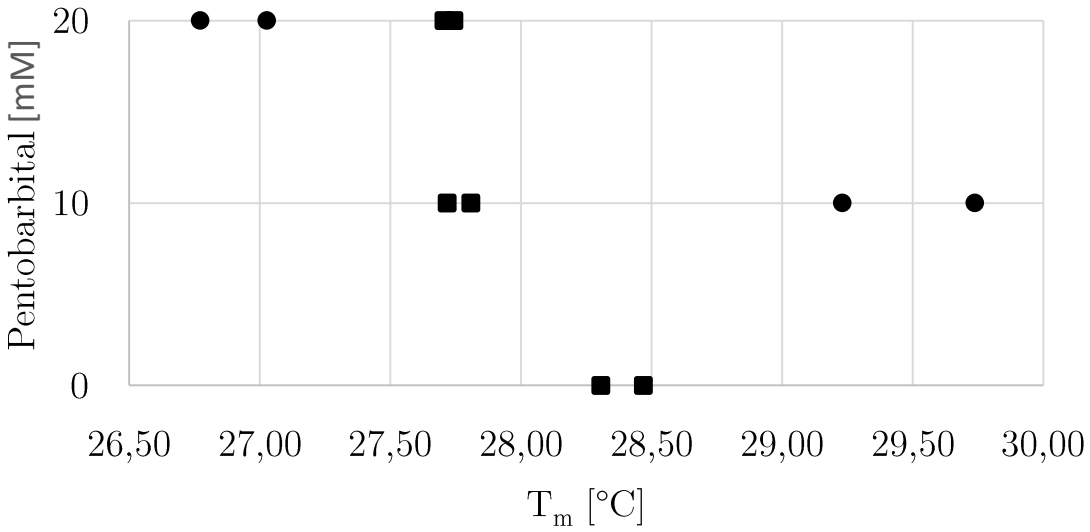

Figure 35: Melting temperature value (peak value) of the each sample was plotted against the amount of mM of the pentobarbital in the sample. Pairs of two data points belong to the same scan and represent the peak values of two consecutive profiles of that scan. Dots represent peak temperatures of profiles produced immediately after the sample had been prepared and square data points represent second scan of the same preparation done 2 or 3 days later. It should be noted that independent variable on the graph is temperature. The axes have been switched for easier comparison

From Figure 33, Figure 34 and graph at Figure 35 it can be seen that pentobarbital has an effect on the melting transition of the lipids. Mixing of pentobarbital with the lipids in the sample occurs over time and between the scans. Time effect gives 3° to 4°C difference between peaks while those of the scans are mostly lower than 1°C.

Unlike sheep spinal cord samples, pig ones have been run over the longer period of time and were mixed with glycerol in order to expand the scanning region. Potential effect of those two parameters are discussed further in the text.

6.3.2. Aging of the sample

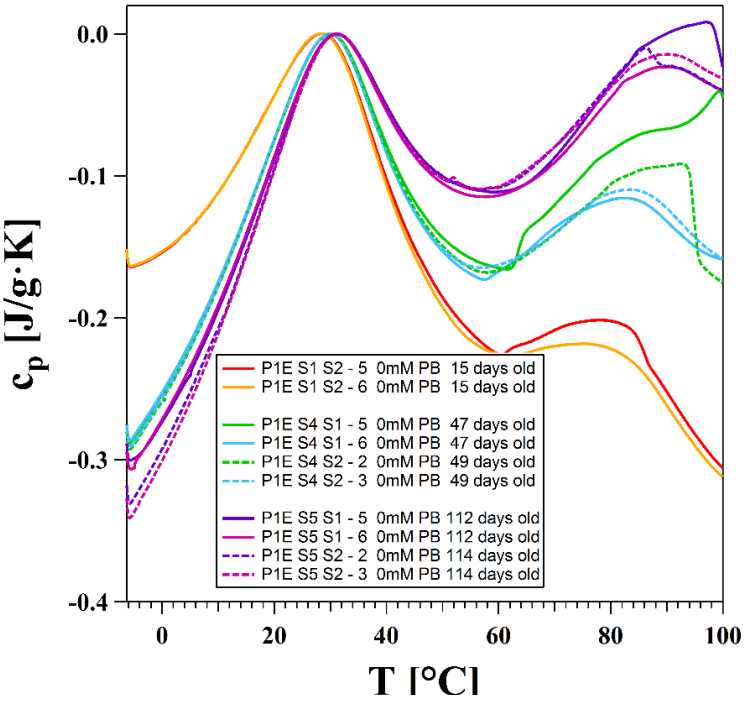

Figure 37: The pig spinal cord sample has been scanned at different times to explore the effect of sample aging on the heat capacity profile. (offset: zero at the lipid peaks)

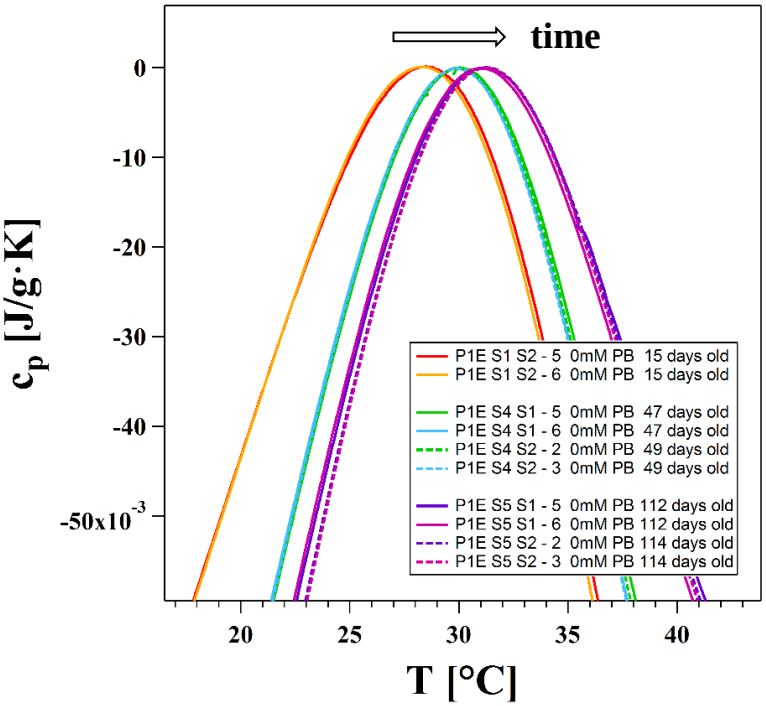

Figure 36: Zoom onto the lipid peak on Figure 37

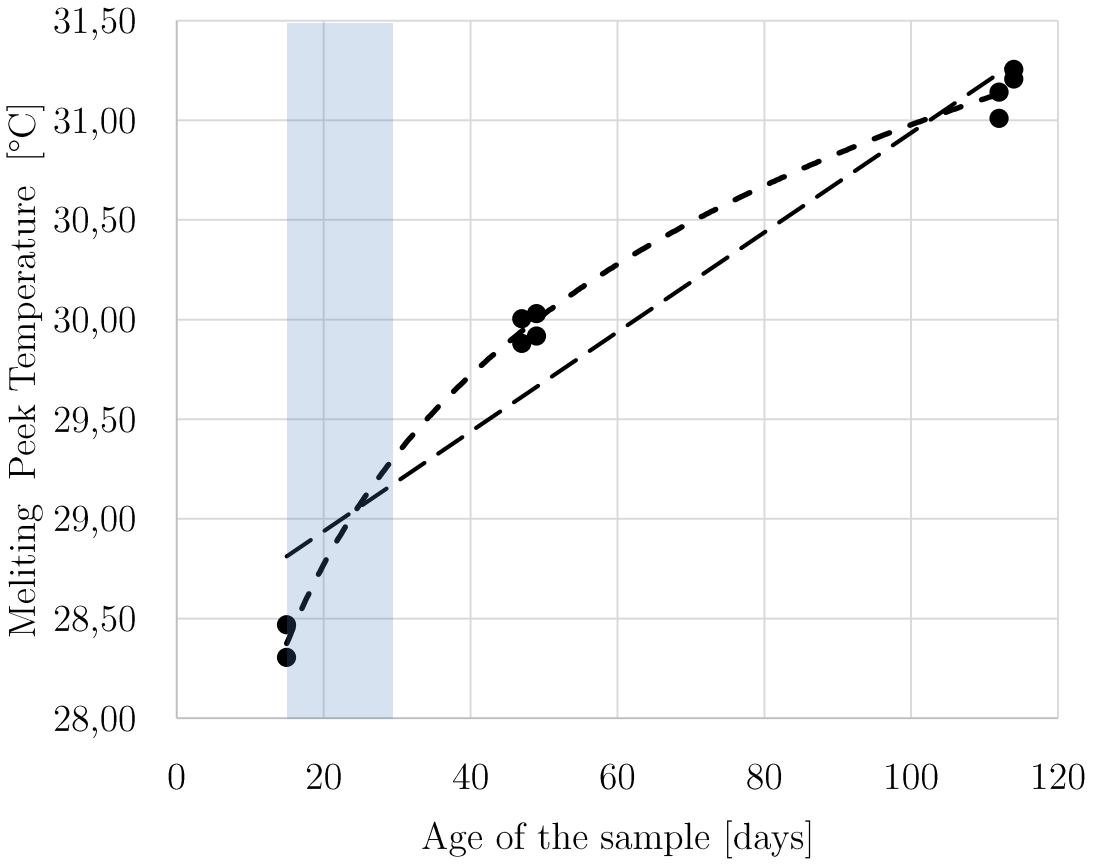

Figure 38: Peak value of the lipid transition at different times. The colored area marks the time frame in which the pentobarbital experiments were done. Aging process shifts the melting transition to higher temperatures. Day 0 is the day of the slaughter.

Aging of the sample rises the lipid peak temperature. Graphs in Figure 37 "tilt" as well as the peak, around 80°C, becomes more pronounced (further in the text it will be shown that that peek seems to be second lipid peak). The sample has been stored in the fridge in a water-based buffer solution which enables the process of oxidation to occur. Oxidation breaks conjugated double bonds in the lipid tails. That process is likely to be the source of the shift. Various empirical rate laws describe oxidization of different substances. Depending on the fit of the data in the Figure 38, lipids in pentobarbital experiments could have been affected by aging process anywhere from less than 0.5° (linear fit) to less than 1.5°C (logarithmic fit).

6.3.3. Lipid extraction

In Figure 39 it can be seen that extracted lipids from the sample have a similar heat capacity profile as the whole sample when it has reached equilibrium. This confirms that the effects that have been studied so far are indeed the effects on lipids in the sample. Extracted lipids also age in the same manner as the rest of the sample, independent of the time when they were extracted. P1E S5 scans follow more closely the shape of the extracted lipids scan, although the extraction process itself has been done closer to the dates when P1E S4 scans were recorded. Lipids give two broad lipid transitions, first around 30°C and the second one at higher temperatures, around 80°C. This profile has similar features to one of the synthetic lipids mixtures. [30] Mixtures of lipids influence positions of transition peaks. The fact that this sample consists of many different lipid species does not exclude the existence of multiple phase transition peaks, below and above temperature region that has been scanned.

There is also a sharp peak at 51,5°C that has been observed only in the extraction scan, with the exception of the very last full sample scan, P1E S5 S2 seen in Figure 39 in blue.

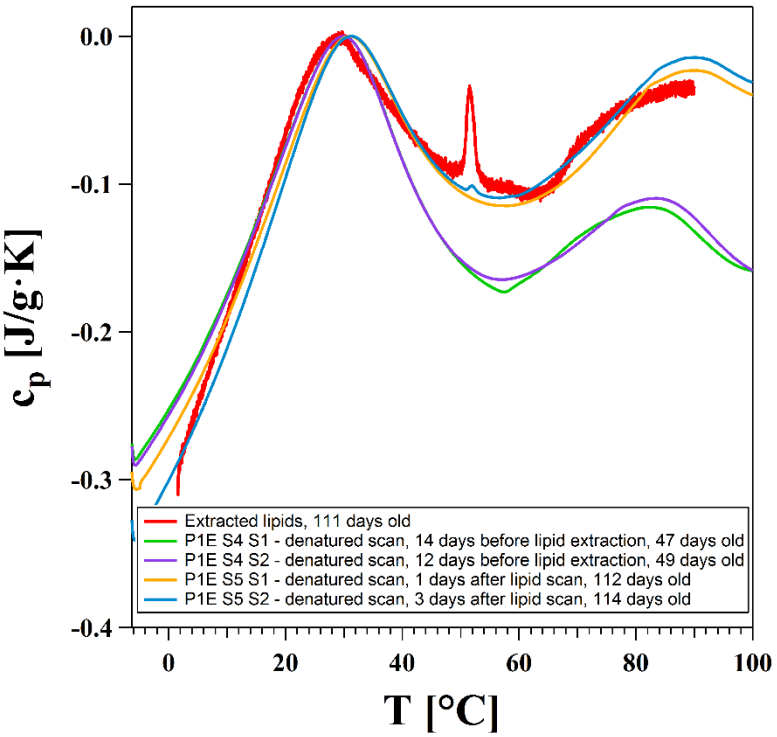

Figure 39: Extracted lipids (red) heat capacity profile compared to the full sample scans at relevant age. (offset: zero at the lipid peaks)

6.4 The effect of glycerol

Having glycerol in the pig spinal cord sample enabled exploring wider temperature range of the heat capacity profile. By running the DPPC samples at similar conditions as the pig spinal cord samples, we wanted to investigate whether the glycerol has an effect on the lipids and the heat capacity of the transition.

Figure 40 shows that glycerol raises and broadens the lipid peak. For 30 wt. % of glycerol that has been added to the buffer, the transition shifts by 0.5°C. This means that the position of a lipid peaks in the biological samples could have been affected as well. However, since all the biological samples were exposed to the same amount of glycerol potential shift should not affect the relative changes when scans are being compared.

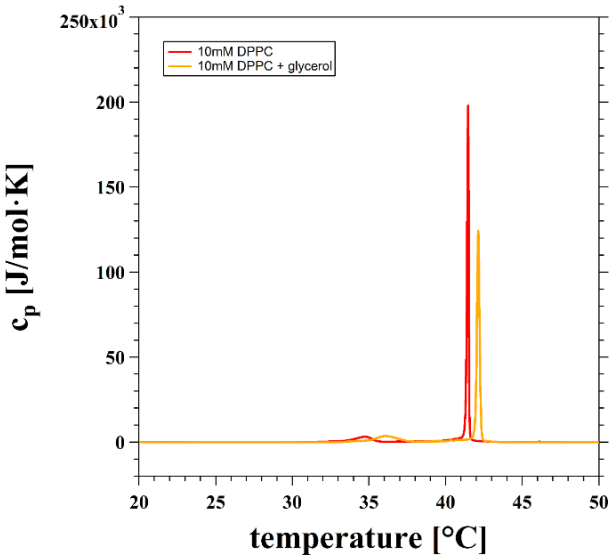

Figure 40: Excess heat capacity of the phase transition in DPPC-MLV in phosphate buffer and in phosphate buffer with added glycerol.

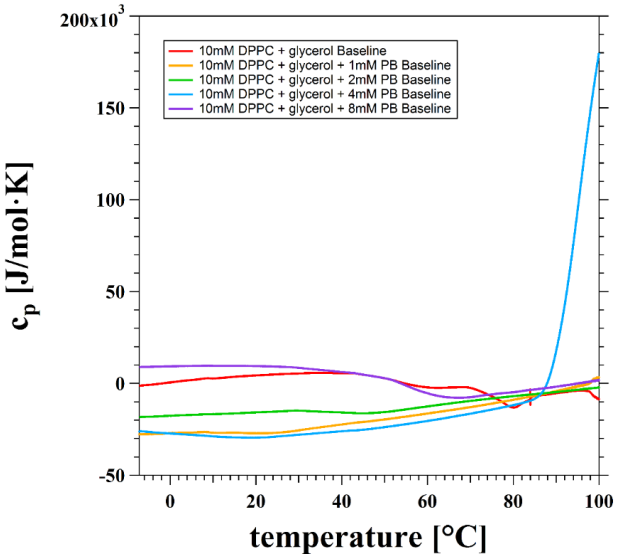

Figure 41: Baselines of buffer with glycerol. The lipid peaks have been deducted from the scans.

As it could be seen in Figure 41 the baselines in the presence of glycerol are not constant, which could cause variations between profiles. Although glycerol has enabled us to investigate the profile in wider temperature range, biological samples have weak profiles compared to those of synthetic lipids and thus introducing additional substances, like glycerol should be avoided.

7 Conclusion

The intention of this thesis was to investigate, for the first time, the influence of anesthetics on the complex phase transitions in biomembranes. A big part of this thesis was dedicated to the development and the optimization of methods for sample preparation. Obtained results show that anesthetics change the membrane properties by shifting the gel fluid phase transition of the lipids. According to the Soliton model the nerve pulse is described as a density pulse. Changing the properties of the membrane thus changes the conditions for the nerve pulse to be created. The results presented in this thesis support the assumptions of the Soliton model and are in agreement with previous work done on synthetic membranes. Additionally, the heat

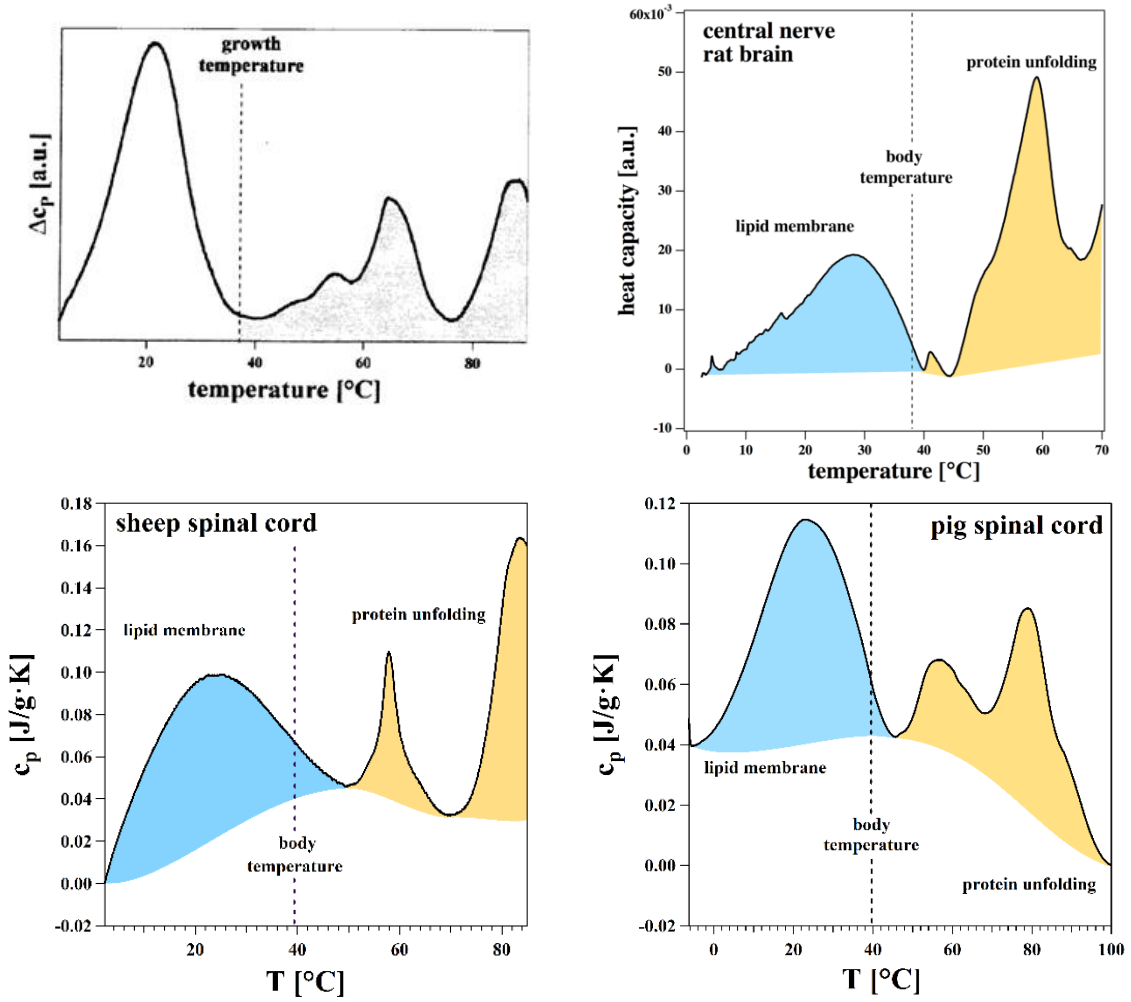

Figure 42: Heath capacity profiles of the E-coli profile [1] (top left), rat brain profile [18] (top right), sheep spinal cord (bottom left) and pig spinal cord (bottom right). The first part of the excess heat capacity is reversible and thus contributed to the change in the phrase of the lipid membrane. Membrane melts transferring from gel phase into fluid phase. In higher temperature regions excess heat capacity records unfolding and aggregation of the proteins. End of the lipid transition seems to be closely related to the body temperature of an organism or in the case of e-coli the growth temperature.

capacity profiles of both sheep and pig spinal cord have similar features to those of e-coli and rat brain that have been investigated previously in our group (Figure 42).

IDEAS FOR FUTURE WORK

The focus of this thesis has been primarily to investigate predictions proposed by the Soliton model in the context of nerve signal propagation. Apart from exploring the predictions of the Soliton model in the biological system and comparing it with already known findings in synthetic lipid membranes, like pressure reversal of the anesthesia [31], it would be interesting to investigate how this approach could be used in medicine. Since lipids are a building blocks of all membranes, both cell walls and the membranes of the organelles, their state is crucial for the normal function of the biological system.

At the time of handing in this thesis our group began an interesting collaboration with the Center for Experimental Drug and Gene Electrotransfer at Herlev Hospital headed by Julie Gehl. Their main focus is investigating means of effective transport of drugs to cancer tissue using the technique of electroporation. Electroporation increases the permeability of the cell membrane if an electrical field is applied to it. This allows drugs to be introduced into the cancerous cells.

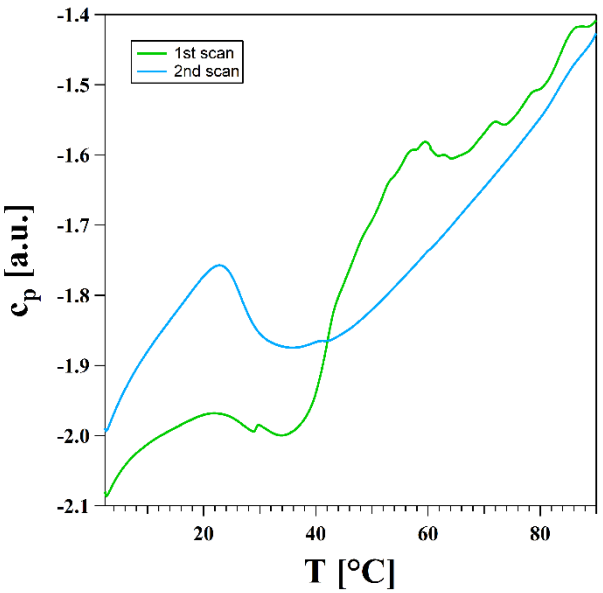

Figure 43: Raw data of a preliminary DSC scan of extracted membranes from colon cancer cells (HT29). In the 1st scan it is possible to see the unfolding of proteins at high temperatures. In the 2nd scan the protein peaks now disappear due to irreversible unfolding of proteins. The lipid peak stays the same, with a somewhat higher amplitude.

As the Soliton model proposes, both growth temperature (of the cells) or body temperature (of the organisms), as well as chemicals dissolved into the structure can influence the phase behavior of lipids at a certain temperature. [8] These and other thermodynamic parameters have to be taken into account if we want to take advantage of the certain properties of the membranes.

In collaboration with the group at Herlev Hospital, we have started a new line of experiments where colon cancer cells (HT29) are going to be exposed to various

amount of calcium. (Figure 43) Calcium is expected to increase the melting temperature of the lipids as it favors the gel phase.

Another interesting phenomenon that could be investigated is the heartbeat. Heart muscle cells work by contraction. Contraction requires electrical/chemical stimulation, is followed by a refractory period and the cells produce electrical pulses that stimulate neighbors. (Figure 44) Moreover, insulin secretion in healthy patients works in pulsatile manner as well with a similar feedback loop. These stages of signal propagation are qualitatively very similar to the one of a nerve.

Both in hearth and in pancreas, calcium bursts throughout the tissue are responsible for the contraction and secretion, respectively. This positive feedback mechanism is called Calcium induced calcium release (CIRC). Although mainly used to explain depolarization across the cell membrane, membrane thickening caused by the calcium induced phase shift in the membrane could play an important role in the mechanism of physical contraction of the cell itself as the gel lipid phase requires less area and volume.

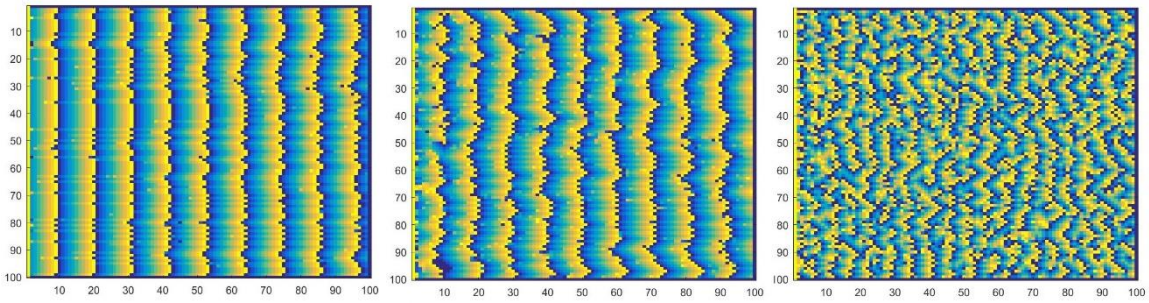

Figure 44: The Matlab simulation I did of a heartbeat propagation model [37] as a part of Physics of diseases course. Each pixel in 100 x 100 panel represents a hart cell. As the wave fronts encounter dysfunctional cells (left), fronts get distorted (middle) which eventually causes self-enforcing loops (right) that could be recorded as cardiac arrhythmia. If the calcium bursts through the tissue are directly connected to the contraction by changing the phase of the membrane, it would be interesting to investigate if the dysfunctional cells could be treated by changing thermodynamical properties of their membranes instead of invasive surgery treatments or pacemakers.

Bibliography

[1] T. Heimburg, *Thermal Biophysics of Membranes*, First edit. Wiley-VCH, 2007.

[2] T. Heimburg, "Lipid ion channels," *Biophys. Chem.*, vol. 150, no. 1–3, pp. 2–22, 2010.

[3] P. Morell and R. H. Quarles, "Characteristic Composition of Myelin." Lippincott-Raven, 1999.

[4] O. G. Mouritsen and M. Bloom, "Mattress model of lipid-protein interactions in membranes.," *Biophys. J.*, vol. 46, no. 2, pp. 141–153, 1984.

[5] T. Heimburg, "A model for the lipid pretransition: coupling of ripple formation with the chain-melting transition," *Biophys. J.*, vol. 78, no. March, pp. 1154–1165, 2000.

[6] T. Heimburg, "Mechanical aspects of membrane thermodynamics. Estimation of the mechanical properties of lipid membranes close to the chain melting transition from calorimetry," *Biochim. Biophys. Acta - Biomembr.*, vol. 1415, no. 1, pp. 147–162, 1998.

[7] A. L. Hodgkin and A. F. Huxley, "A quantitative description of membrane current and its application to conduction and excitation in nerve," *Bull. Math. Biol.*, vol. 52, no. 1–2, pp. 500–544, 1952.

[8] T. Heimburg and A. D. Jackson, "On soliton propagation in biomembranes and nerves.," *Proc. Natl. Acad. Sci. U. S. A.*, vol. 102, no. 28, pp. 9790–9795, 2005.

[9] I. Tasaki and K. Iwasa, "Temperature changes associated with nerve excitation: Detection by using polyvinylidene fluoride film," *Biochem. Biophys. Res. Commun.*, vol. 101, no. 1, pp. 172–176, 1981.

[10] K. Iwasa and I. Tasaki, "Mechanical changes in squid giant axons associated with production of action potentials.," *Biochem. Biophys. Res. Commun.*, vol. 95, no. 3, pp. 1328–1331, 1980.

[11] B. Lautrup, R. Appali, a D. Jackson, and T. Heimburg, "The stability of solitons in biomembranes and nerves.," *Eur. Phys. J. E. Soft Matter*, vol. 34, no. 6, pp. 1–9, 2011.

[12] K. Graesbøll, H. Sasse-Middelhoff, and T. Heimburg, "The thermodynamics of general and local anesthesia.," *Biophys. J.*, vol. 106, no. 10, pp. 2143–56, May 2014.

[13] C. E. Overton, *Studien über die Narkose, zugleich ein Beitrag zur allgemeinen Pharmakologie*. Jena, Germany: Fisher, 1901.

[14] H. Meyer, "Zur Theorie der Alkoholnarkose. Erste Mittheilung. Welche Eigenschaft der Anästhetica bedingt ihre narkotische Wirkung?," *Arch. für Exp. Pathol. und Pharmakologie*, pp. 109–118, 1899.

[15] D. P. Kharakoz, "Phase-transition-driven synaptic exocytosis: A hypothesis

and its physiological and evolutionary implications," *Biosci. Rep.*, vol. 21, no. 6, pp. 801–830, 2001.

[16] Marven, "Microcal DSC Systems Understanding Biomolecular Stability." Malvern Instruments Limited, Worcestershire, p. 16, 2015.

[17] F. Tounsi, "The Correlation Between Critical Anesthetic Dose and Melting Temperatures in Synthetic Membranes," University of Copenhagen, 2015.

[18] S. M. Madsen, "Thermodynamics of nerves," University of Copenhagen, 2011.

[19] "Lister over autoriserede fødevarevirksomheder/Lists of approved food plants." [Online]. Available: https://www.foedevarestyrelsen.dk/fvst_ansvar_opgaver/Sider/Lister_over_autoriserede_f%C3%B8devarevirksomheder.aspx. [Accessed: 16-May-2016].

[20] R. N. Goldberg, N. Kishore, and R. M. Lennen, "Thermodynamic quantities for the ionization reactions of buffers," *J. Phys. Chem. Ref. Data*, vol. 31, no. 2, pp. 231–370, 2002.

[21] "Isothermal Titration Calorimetry Page - Department of Biochemistry, University of Oxford." [Online]. Available: http://www.bioch.ox.ac.uk/aspsite/index.asp?pageid=496. [Accessed: 24-May-2016].

[22] S. O. Ugwu and S. P. Apte, "The Effect of Buffers on Protein Conformational Stability," *Pharm. Technol.*, vol. 28, no. 3, pp. 86–109, 2004.

[23] D. S. Prough and A. Bidani, "Hyperchloremic metabolic acidosis is a predictable consequence of intraoperative infusion of 0.9% saline.," *Anesthesiology*, vol. 90, no. 5, pp. 1247–9, May 1999.

[24] M. F. Rothschild and A. Ruvinsky, *The Genetics of the Pig*. CABI, 2010.

[25] D. Burden, "Guide to the homogenization of biological samples," *Random Prim.*, no. 7, pp. 1–14, 2008.

[26] A. a. Chagovetz, C. Quinn, N. Damarse, L. D. Hansen, A. M. Chagovetz, and R. L. Jensen, "Differential scanning calorimetry of gliomas: A new tool in brain cancer diagnostics?," *Neurosurgery*, vol. 73, no. 2, pp. 289–295, 2013.

[27] D. R. Lide, *Handbook of Chemistry and Physics*, 88th editi. Boca Raton, FL: CRC Press, Taylor & Francis, 2007.

[28] W. J. Bligh, E.G. and Dyer, "Canadian Journal of Biochemistry and Physiology," *Can. J. Biochem. Physiol.*, vol. 37, no. 8, 1959.

[29] J. A. Dean, *Lange's Handbook of Chemistry*, 10th editi. New York: McGraw-Hill, 1967.

[30] H. M. Seeger, M. Fidorra, and T. Heimburg, "Domain size and fluctuations at domain interfaces in lipid mixtures," *Macromol. Symp.*, vol. 219, pp. 85–96, 2004.

[31] T. Heimburg and A. D. Jackson, "The thermodynamics of general anesthesia.," *Biophys. J.*, vol. 92, no. 9, pp. 3159–3165, 2007.

[32] L. D. Mosgaard, "The Electrical and Dynamical Properties of Biomembranes,"

University of Copenhagen, 2014.

[33] "The Cell Membrane - Anatomy & Physiology - OpenStax CNX." [Online]. Available: http://cnx.org/contents/FPtK1zmh@6.27:q2X995E3@6/The-Cell-Membrane. [Accessed: 25-Apr-2016].

[34] F. Becher, "The Relation Between Enthalpy And Volume Change," University of Copenhagen, 2014.

[35] E. N. Marieb and K. Hoehn, *Human Anatomy & Physiology*. Pearson Benjamin Cummings, 2007.

[36] M. Frei, "Centrifugation," *Sigma-Aldrich*, vol. 6, no. 5, pp. 17–21, 2014.

[37] K. Christensen, K. A. Manani, and N. S. Peters, "Simple model for identifying critical regions in atrial fibrillation," *Phys. Rev. Lett.*, vol. 114, no. 2, pp. 1–6, 2015.